Master thesis

Climate risk and vulnerability assessment tool

Date : 01.09.2023

Laboratory: Extreme Environments Research Laboratory (EERL)

Author

Camille Dross

EPFL Supervisor

Prof. Dr. Julia Schmale

COWI Supervisors

Dr. Raphael Payet-Burin

Dr. Silvio Pereira

Abstract

Changing climatic conditions and increase of extreme events induced by climate change have impacts on non-adapted infrastructures, leading to destruction, damage costs and indirect impacts. To adapt infrastructures to those new conditions, there is a need to identify vulnerabilities and risks due to climate change. To that end, a Climate Risk and Vulnerability Assessment tool was designed based on 'Non-paper Guidelines for Project Managers: Making vulnerable investments climate resilient' proposed by the European commission. It relies on three steps: vulnerability assessment, risk assessment and climate mitigation. The tool was applied in a water treatment plant project located in Gorongosa, Mozambique. The climate projections used for the application of the tool are part of NEX-GDDP-CMIP6 dataset. Produced by NASA, this set of modelled data results from the bias-correction with quantile mapping and downscaling of the CMIP6 dataset. Comparing them to historical observed data revealed that average temperatures did match in trend, mean and extremes. However, the trends of the historic modelled maximum temperature were higher than the observed ones. Moreover, modelled precipitation did not match the observed distribution for high and extreme values. Therefore, the bias correction method quantile mapping was performed on those two modelled climate variables to diminish the biases. It performed well on maximum temperature data; the bias correction output complied much more with observation data than raw data. However, for precipitation data, extreme precipitation events biases corrected were much lower than the observed data and were all similar between models. To better capture the behavior of precipitation, it is recommended to use parametric distributions for mapping instead of non-parametric ones, as it was done in this study. Because of unverified compliance of the biases to the stationarity assumption and inconclusive results of bias-corrected precipitation, the raw NEX-GDDP-CMIP6 data with its biases were used to apply the tool at Gorongosa. The application of the tool permitted to learn about the climate evolution at this location. According to NEX-GDDP-CMIP6 and CORDEX (Coordinated Regional Climate Downscaling Experiment) results, a general increase of the temperature is projected in Gorongosa for future years. The precipitation projections agree on a decrease in average precipitation, but an increase for extreme events at Gorongosa. The tool also permitted to highlight the vulnerability of pumps and of the switchgear of the water treatment plant in Gorongosa to extreme air temperature increase. The sensitivities of other project's elements were also pointed up thanks to the tool, such as the sensitivity of rapid sand filter, pumps, and transformers to increasing air temperature. Some technical solutions exist and should therefore be applied to reduce the sensitivity and contribute to decrease the vulnerability of the project. The tool could be refined in its categorization approach and by imposing different thresholds, depending on the climate variable studied.

Abstract French version

L'évolution des conditions climatiques et l'augmentation des événements extrêmes induits par le changement climatique ont des répercussions sur les infrastructures non adaptées, entraînant des destructions, des coûts et des impacts indirects. Pour adapter les infrastructures à ces nouvelles conditions, il est nécessaire d'identifier les vulnérabilités et les risques liés au changement climatique. À cette fin, 'Climate Risk and Vulnerability Assessment tool' – un *outil d'évaluation des risques climatiques et de la vulnérabilité*- a été conçu sur la base du 'Non-paper Guidelines for Project Managers : Making vulnerable investments climate resilient' ("*Lignes directrices pour les gestionnaires de projet : Rendre les investissements vulnérables résilients au changement climatique*") proposé par la Commission européenne. Il repose sur trois étapes : l'évaluation de la vulnérabilité, l'évaluation des risques et l'identification de mesures pouvant atténuer la vulnérabilité et le risque. L'outil a été appliqué à un projet de station d'épuration situé à Gorongosa, au Mozambique. Les projections climatiques utilisées pour l'application de l'outil font partie de l'ensemble de données NEX-GDDP-CMIP6. Produit par la NASA, cet ensemble de données modélisées résulte de la correction des biais avec la méthode de quantile mapping -*cartographie des quantiles*- et de downscaling -*réduction d'échelle*- de l'ensemble de données CMIP6. En les comparant avec les données historiques observées, il a été mis en évidence que les températures moyennes correspondaient en termes de tendance, de moyenne et d'extrêmes. Cependant, les tendances des températures maximales historiques modélisées étaient plus élevées que les températures observées. De plus, les précipitations modélisées ne correspondaient pas à la distribution observée pour les valeurs élevées et extrêmes. Afin de réduire les biais, la méthode de correction des biais par cartographie des quantiles a été appliquée à ces deux variables climatiques modélisées. Cette méthode a donné de bons résultats pour les données de températures maximales ; les résultats de la correction des biais correspondaient beaucoup plus aux données d'observation que les données brutes. Cependant, les données de précipitations corrigées étaient plus basses que les données observées et les extrêmes étaient tous similaires entre les modèles. Pour mieux saisir le comportement des précipitations, il est recommandé d'utiliser des distributions paramétriques pour la cartographie des quantiles (quantile mapping) plutôt que des distributions non paramétriques, comme cela a été fait dans cette étude. La conformité des biais à l'hypothèse de stationnarité n'ayant pas été vérifiée et les résultats de la correction des biais des données de précipitations étant non concluants, les données brutes NEX-GDDP-CMIP6, avec leurs biais, ont été utilisées pour appliquer l'outil à Gorongosa. L'application de l'outil a permis de connaître l'évolution du climat à cet endroit. Selon les résultats de NEX-GDDP-CMIP6 et de CORDEX (Coordinated Regional Climate Downscaling Experiment - *Expérience régionale coordonnée de réduction d'échelle du climat*), une augmentation générale de la température est prévue à Gorongosa pour les années à venir. Les projections de précipitations s'accordent sur une diminution des précipitations moyennes, mais une augmentation des événements extrêmes à Gorongosa. L'outil a également permis de mettre en évidence la vulnérabilité des pompes et de l'appareillage de commutation électrique de la station de traitement des eaux de Gorongosa à une augmentation extrême de la température de l'air. Les sensibilités d'autres éléments du projet ont également été mises en évidence grâce à l'outil, comme la sensibilité à l'augmentation de la température de l'air du filtre à sable rapide, des pompes et des transformateurs. Certaines solutions techniques existent et devraient donc être appliquées pour réduire la sensibilité et contribuer à diminuer la vulnérabilité du projet. L'outil pourrait être affiné dans son approche de catégorisation et en imposant différents seuils, en fonction de la variable climatique étudiée.

Contents

List of figures

List of tables

List of codes

All code listed below are on this Github.

Code 1: CRVA_data_analyst contains the CRVA tool

Code 2: Download_NEX-GDDP-CMIP6

Code 3: CSV_NEX-GDDP-CMIP6_one_lat_lon

Code 4: CSV_Obs_NEXGDDPCMIP6_one_lat_lon

Code 5: Compare NOAA station and NEXGDDP CMIP6 data in Chimoio

Code 6: Treat Data tas NOAA Station and pr meteorological station gorongosa

Code 7: BC_NEX-GDDP-CMIP6

Code 8: Bias_correction_function

Code 9: Functions_ImportData

Code 10: Functions_Indicators

Code 11: Functions_likelihood

List of abbreviations

BC: Bias correction

BCSD: Bias Correction Spatial Disaggregation

CMIP6: Coupled Model Intercomparison Project Phase 6

CDF: Cumulative Distribution Function

CORDEX: Coordinated Regional Climate Downscaling Experiment

CRVA: Climate Risk and Vulnerability Assessment

DQM: Detrended Quantile Mapping

EIB: European Investment Bank

ENSO: El Niño-Southern Oscillation

FIPAG: Fundo de Investimento e Património do Abastecimento de Água - *Water Supply Equity and Investment Fund*

GCM: General Circulation Model

GHCNd: Global Historical Climatology Network daily

GHG: Greenhouse gases

GMFD: Global Meteorological Forcing Dataset

IPCC: Intergovernmental Panel on Climate Change

NASA: National Aeronautics and Space Administration

NEX-GDDP-CMIP6 : NASA Earth Exchange (NEX) Global Daily Downscaled Projections (GDDP) Coupled Model Intercomparison Project Phase 6

NOAA: National Oceanic and Atmospheric Administration

QDM: Quantile delta mapping

QM: Quantile mapping

RCP: Representative Concentration Pathway

SDM: Scaled Distribution Mapping

SSP: Shared Socioeconomic Pathways

WMO: World Meteorological Organization

WTP: Water treatment plant

Acknowledgements

I would like to give particular thanks to Raphael Payet-Burin, who was my first contact at COWI and suggested this topic of thesis. Thanks as well to Raphael Payet-Burin and Silvio Pereira, for their supervision along the project, for the time and attention they dedicated to this project, and for re-motivating me during more difficult moments. It was a pleasure having them as colleagues and supervisors for a few months.

Thanks as well to the firm COWI, and to all my colleagues in the Global advisory department; I felt immediately integrated in the team. My work was helped by this feeling.

Thanks to Julia Schmale for her precious advices and the time she dedicated to supervise this thesis.

On a more personal note, I would like to thank my friends at EPFL, who became my second family and permitted me to go through the few difficult, but pleasant, academic years. A special thanks to my parents, who always believed in my abilities, and encouraged me through all my studies and efforts.

1 Introduction

Since the mid-20th century, climate is changing due to anthropogenic emissions (1,2). Several key indicators of the climate have shifted, such as the global temperature which is increasing (1). Higher intensity and frequency of extreme events have been observed since the pre-industrial time in temperature extremes, heavy precipitations and floods, drought, and storms (3,4). According to projections, those changes will continue (5). The impacts of climate change affect natural, human, and managed systems (6). As part of human systems, infrastructure can be affected (6).

For example, increasing rainfall associated with tropical cyclones and rising sea levels contributes to observed damages on the coasts (6). In 2014, a part of the mainline railway at Dawlish, in Devon, UK was affected by coastal flooding. As this section was considered important, it was repaired quickly, at a cost estimated at £40-45 million (7). Another impact of climate change on railway occurs during heat waves; rails are submitted to thermal expansion of their steel structure. In 2019, in UK, several trains were travelling on tracks with a lower speed, to avoid derailments (7). Some impacts are less impressive and slower. This could be illustrated with the thaw of permafrost, due to increasing temperatures. It could affect around 30 to 50% of critical circumpolar infrastructure by 2050 (8). The potential damage cost of permafrost thaw is estimated up to tens of billions of US dollars for the second half of this century (8,9). Another case is the growth of carbonation-induced corrosion due to the increase of atmospheric CO2, leading to an acceleration of concrete infrastructure erosion (10). The impacts of climate change on infrastructures are causing degradation of infrastructures and damage costs. However, some impacts of climate change can also be indirect. Roads are vulnerable to climate change as they are exposed to environmental conditions. But they are related to economic growth, development, and social welfare, which could be threaten by unusable roads (11). Some other impacts of climate change affect other domains, on which the current society relies. This can be seen in Mozambique, with hydropower. This is the main source of electricity in Mozambique. However, precipitation has generally been decreasing and the temperature has been increasing within the country during the last decades. This leads to less water in rivers and less energy production with hydropower, while Mozambique is facing an increasing demand for electricity (12).

Climate impacts directly affected infrastructures, and through them, the economy, and other fields such as energy. As infrastructures and networks are essential to the functioning of the society, Intergovernmental Panel on Climate Change (IPCC) identified the risk to critical physical infrastructure and networks as a key risk. In the sixth report of IPCC, risk is defined as the potential for adverse consequences for human, or ecological systems. It is shaped by hazard, vulnerability, and exposure (6).

Those concepts are currently used for many climate risk assessments (7,13), to identify sectors at risk and therefore find adapted solutions (14). A methodology from the European Commission aims to help project managers to make investment projects climate resilient, to identify risks for a project and implement climate mitigation if needed (15,16).

This methodology is applied in the context of a COWI project. COWI is an engineering and architecture consultancy group, involved in many infrastructure projects[1]. The team 'Studies and Investment Implementation' of the Global Advisory department is in charge to assist technically the Project Preparation and Implementation Support (PPIS) to the Mozambique Climate Resilient Framework Loan. The client is the European Investment Bank (EIB). COWI must give a support to the Mozambican Water Authorities Fundo de Investimento e Património do Abastecimento de Água (FIPAG) - *Water Supply Equity and Investment Fund*-, to rebuild climate-proof water infrastructures that were damaged by the cyclones in 2019 across the country. Those cyclones named Idai and Kenneth affected the country within a few weeks, in March and April 2019 (17). The

[1] COWI webpage

estimated cost of damages caused to agriculture, infrastructure and buildings by cyclone Idai is 773 million US$ (18). To properly assess risks and rebuild infrastructure resilient to climate change, a project of Climate Risk and Vulnerability Assessment (CRVA) tool applying the method of the European Commission has emerged, financed by COWI Foundation (19,20). The aim is to develop a tool to estimate climate risks for infrastructure projects. As COWI is implicated in infrastructure projects, this could also be useful for other departments.

In the light of the precedent elements, how to assess risks due to/influenced by climate change on infrastructures of on-going projects? How to summarize hazards and risks due to/influenced by climate change on the infrastructures and urban planning of on-going projects and on agriculture?

2 Methods and materials

2.1 Study area

Mozambique is an African country located on the South-East coast of the continent. The climate is semi-arid and subtropical in the south, and tropical in the north. It is characterized by two seasons. The first one is the wet/rainy season from October to March (12). Most cyclones are experienced during this period. The highest rainfall amount is observed between December and March (21). The second season is the dry one from April to September. Droughts are more frequent during that period of the year. Because of its tropical climate, temperature variations between seasons and within seasons are small in comparison to other climates (21). Between 1991 and 2021, the average annual mean temperature varied between 24 and 25°C, the average seasonal maximum temperature reached in the country was around 31°C and the average seasonal minimum was around 12°C (22). Precipitation across the country and the season varies more. The annual average precipitation is 1032 mm, varying between 2000 mm/year in the mountainous part of the country, to 300 mm/year in the South (12).

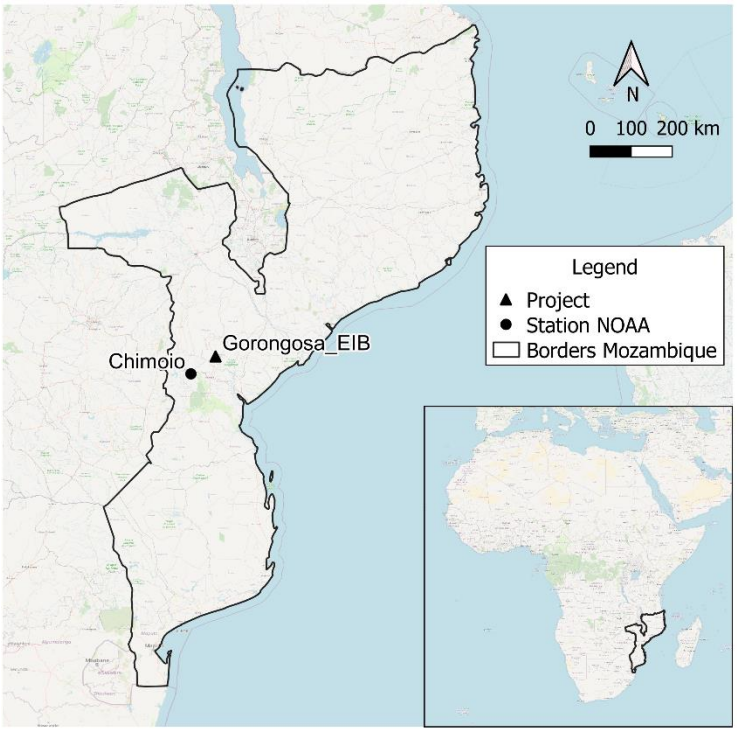

Figure 2-1 - Map of Mozambique, presenting COWI's project in Gorongosa on which the method was applied, with the NOAA meteorological station in Chimoio with which modeled data are compared. The background of the map is OSM Standard, and the projection of the map is WGS 84 EPSG:4326. The map was done with QGIS

Mozambique is one the African countries most prone to related hazard weather, such as cyclones, floods, or drought (18,21,23). According to climate change studies, droughts and floods will increase mostly in the tropical part, where Mozambique is located (12). Currently, the country does not have the financial resources and infrastructures to cope with those changes, which also makes this country one of the most vulnerable to climate change (12,23). According to the World Meteorological Organization (WMO), the 2019 cyclones recalled the necessity to make Mozambique more resilient to climate change (18).

To identify project elements who could be affected by climate change and the climate-linked risk, the tool was applied on one sub-project of the 'Mozambique EIB Project Preparation and Implementation Support for Climate Resilient Framework Loan, showed in with a black triangle in Figure 2-1. The sub-project is in Gorongosa. The

scope of this project is to build an extension to the existing water treatment plant (WTP), to increase its capacity. Moreover, works should be done on the existing infrastructure. All those works should be resilient to climate change afterwards. Information concerning the project comes from internal COWI documents.

The point on Figure 2-1 is the location of the meteorological station from National Oceanic and Atmospheric Administration (NOAA), from which observation data will be used later in this report.

2.2 Climate models and predictions

Evaluate impact of climate change leads to use some definitions set by the Intergovernmental Panel on Climate Change (IPCC). This is an intergovernmental body of the United Nations which aims to produce assessment reports about the current scientific, technical, and socio-economic knowledge on climate change and its consequences. The report also presents solutions to reduce impact of climate change (24). To write those reports, the IPCC developed a set of notions that are used in this master thesis report.

Climate is the average weather over a period going from months to millions of years of the climate system. This last one is composed of atmosphere, hydrosphere, cryosphere, lithosphere, and biosphere. Over time, the climate system varies due to its own dynamic and due to external forcings (example: volcanoes). To describe the current state of the climate system and to know more about climate, some quantities are used, such as near surface temperature or precipitation. Those quantities are climate variables (25).

To estimate climate in the future, climate projections for each climate variable can be used. They are generally obtained for several General Circulation Models (GCMs) (26) (also called climate models), having as inputs the conditions under specific Shared Socio-economic Pathways (SSPs). GCMs are numerical models representing the climate system and its interactions (25). It produces time series of values for past and future (27). It is used to study the climate system's evolution across time and space (28). GCMs are completed by RCMs (Regional Climate Models) (25). Whereas GCMs covers large regions in the world (all Europe for example), RCMs cover sub-regions of the GCMs (example: Mediterranean basin) with a finer scale (29). RCMs are obtained by dynamical downscaling, with GCMs as inputs (29). GCMs and RCMs are modelled by different institutes around the world (30).

SSPs are scenarios of the potential future, depending on economic, demographic, technological innovation, governance, lifestyles, and relationship hypothesis (28). SSPs are linked to Representative Concentration Pathways (RCPs), which are time series of emissions and concentration of greenhouse gases and aerosols: SSPs indicate the socio-economic conditions for each RCP to happen. SSP abbreviation can indicate two different notions: the socio-economic scenarios families (Figure 2-2) which are just the general hypothesis behind a SSP group, and the emission scenarios. Those ones suppose that a certain effective radiative forcing will be reached at the end of the century (For example SSP1-1.9 suppose 1.9 $W.m^{-2}$ will be reached at the end of the century) (5). Radiative forcing is the change in the energy budget (net radiative flux) at the top of the atmosphere; a positive one induces warming, and a negative one induces cooling (28) (25).

Figure 2-2 – SSP families (31)

In this report, the SSP will only indicate emission scenarios (25). The emission scenarios are written under the form SSPX-Y, X being the number of the socio-economic scenario family to which the emission scenario is complying and Y being the radiative forcing $W.m^{-2}$ reached by 2100. For more simplicity, in this work, they will be written under the form sspXY. In this report, only four emission scenarios will be used: ssp126, ssp245, ssp370 and ssp585 (respectively SSP1-2.6, SSP2-4.5, SSP3-7.0 and SSP5-8.5). The main characteristics of each is summarized in the Table 2-1.

Table 2-1 - Main social, economic and climate policy assumptions, and consequences on greenhouse gases (GHG) emissions for each emission scenarios (28,31)

Emission scenario	Social assumption	Climate policy	Emission pathway
ssp126	SSP1: Sustainable development in the center of policy-making, low consumption and population growth	Climate protection measures implemented	Low GHG emissions scenario: Net zero CO_2 emissions in the second half of the century, permitting to stay below 2°C warming
ssp245	SSP2: no significant shift in comparison to historical social, economic, and technological trends	Climate protection measures implemented	Intermediate GHG emissions scenario: CO_2 emissions staying around current levels, until 2050, where a decrease starts
ssp370	SSP3: a world of rivalry, leading to a slow economic and technological development, and a growing fossil fuel dependency	No additional climate policy	High GHG emissions scenario: Double of CO_2 emissions from current levels by 2100
ssp585	SSP5: International cooperation fully operational, in a world centred on free markets and high consumption.	No additional climate policy	Very high GHG emissions scenario Double of CO_2 emissions from current levels by 2050

Climate projections are often associated to ensembles, which are a set of simulations whose axis members describe how the simulation differs. The simulation can differ because of the realization (r), because of the initialization (i), the perturbation (p), and the forcing (f) (25,32). Only data from the ensemble 'r1i1p1f1_gn' were analyzed in this report.

Projections of future climate rely on models and scenarios. However, the outputs of those models differ. The same radiative forcing is used for all of them, but the numerical methods, mathematical formulas and parametrization vary between all the models, leading to a model uncertainty. As scenarios depend on different population, economic and social development assumptions, projections under those different scenarios also differ. There is a scenario uncertainty. Moreover, without taking in account radiative forcing, the climate has variations, on daily weather, or over decades. Those variations are due to interactions between the components of the Earth system. Some variations are unpredictable due to the chaotic characteristic of Earth's system. Some other can be predicted, such as the El Niño-Southern Oscillation (ENSO) (33). ENSO is a yearly climate variation in the global climate system; interactions between atmosphere and ocean leads to change in ocean circulation (34). These predictable or unpredictable climate variations only due to Earth's component interaction are grouped in the internal variability uncertainty. Therefore, in the climate context, projection uncertainty refers to the different paths of the same climate variable processed by different models and scenarios. The sources of this projection uncertainty are the model uncertainty, the scenario uncertainty, and the internal variability (27). For this thesis, it was decided that projections under every model and every scenario have the same likelihood to occur.

Projections and past modelized data for several climate variables were grouped thanks to the Coupled Model Intercomparison Project (CMIP). This is a program coordinated by the World Climate Research Program (WRCP). It gathers and archives climate model simulations realized with different GCMs, by scientific teams all around the world (25). The Coupled Model Intercomparison Project Phase 6 (CMIP6) datasets can be downloaded, thanks to the work of Copernicus (the Earth Observation component of the European Union's space program) and the European Centre for Medium-Range Weather Forecasts (ECMWF) (35)[2]. Several climate variables modelled with GCMs, for several SSPs and under different ensemble can be downloaded, such as air temperature, precipitation, or relative humidity. Projections with RCMs can also be found thanks to Coordinated Regional Climate Downscaling Experiment (CORDEX)[3].

For this methodology, change of the climate between past and future is done through climate variable changes, such as 'Incremental air temperature change', 'Extreme temperature increase' or 'Incremental rainfall change'. Those climate variables are represented by indicators, to study more precisely the change for a climate variable. For example, an indicator of 'Incremental rainfall change' is 'Average yearly precipitation'. The climate variable changes and indicator studied in this report can be found in Table 2-6, in section 2.5 Methodology of climate risk and vulnerability analysis.

2.3 Climate Data

2.3.1 Observation data

The tool was applied with modelled projection data. Those were compared to observation data, taken from the database Global Historical Climatology Network daily (GHCNd), provided by the National Oceanic and Atmospheric Administration (NOAA) (36). NOAA is a scientific American agency, that aims to understand and predict changes in climate, weather ocean and coasts, and to share their knowledge (37). The database GHCNd provided by NOAA gathers daily climate records from different sources for several climate variables (36,38). In

[2] CMIP6 climate projections (copernicus.eu)
[3] CORDEX regional climate model data on single levels (copernicus.eu)

this report, there is only an interest for the following climate variables: precipitation, temperature, and maximum temperature.

The meteorological station of Chimoio is the closet one to Gorongosa. In the Figure 2-1, the meteorological station is the black point, and the project is the black triangle. Modelled data at the same location and during the same period as the meteorological station data were compared to the observed data from the meteorological station to validate the modelled data. Another set of precipitation observation data is used in this report to validate precipitation data at Gorongosa. They were provided by André Görgens (Consultant, Water resources Management, Zutari) and come from the rainfall measuring station in Gorongosa. The exact coordinates of the measurement are not known.

2.3.2 NEX-GDDP-CMIP6 dataset

Modelled projection data used in this report are all part of the NASA Earth Exchange (NEX) Global Daily Downscaled Projections (GDDP) dataset. It is a set of data produced in 2022 by the NASA (39,40). The aim is to provide a tool to analyze future climate trends and analyze the potential future impacts of those change at a smaller resolution than with GCMs. The climate variables available are the following. Climate variables are almost all available for 35 models and 4 experiments (ssp126, ssp245, spp370 and ssp585) (39).

Table 2-2 - Climate variables available in NEX-GDDP-CMIP6

Short name of the Climate variable	Climate variable	Units
hurs	Near-surface relative humidity	percentage
huss	Near-surface specific humidity	kg/kg
pr	Precipitation (including both liquid and solid phases)	$kg/m^2/s$
rlds	Surface downwelling longwave radiation	W/m^2
rsds	Surface downwelling shortwave radiation	W/m^2
sfcWind	Surface wind speed	m/s
tas	Near-surface air temperature	degrees K
tasmax	Maximum near-surface air temperature	degrees K
tasmin	Minimum near-surface air temperature	degrees K

To obtain the dataset, some outputs from the CMIP6 are first bias-corrected and then downscaled to a 0.25 degree horizontal-resolution (39). Those 2 steps are part of the Bias Correction Spatial Disaggregation (BCSD) method (section 2.4.2 Bias Correction Spatial Disaggregation - BCSD) (Wood 2004).

The method used to bias-correct is quantile mapping. The details about the method, its advantages, and its defaults, can be found in the section 2.4.1. The attention should be raised on two facts for the bias-correction of CMIP6 data to produce NEX-GDDP-CMIP6 data. First, the bias corrected minimum daily temperature is not calculated the same way as the other variables: it is the difference between the bias corrected maximum temperature and the bias-corrected diurnal temperature range fields. Second, it should be noted that the temperature variables are bias corrected slightly differently, by detrended quantile mapping; the GCMs data are detrended before bias-correction. Monthly averages over several years of the climate trends are calculated and is then added back to bias-corrected data. This is performed this way because the BCSD method does not correct explicitly trends (39).

The second step is downscaling (Section 2.4.2 Bias Correction Spatial Disaggregation - BCSD). To produce the NEX-GDDP-CMIP6 dataset, the main action of downscaling is to add the relative changes determined by the GCMs models to the observed historical climate Global Meteorological Forcing Dataset (GMFD). More details on the procedure can be found in Appendix A.

2.3.3 Obtention of NEX-GDDP-CMIP6 data

The data of interest was obtained in two steps: downloading the information, and then reformat the information to use it.

For the first step, code 2 named 'Download_NEX-GDDP-CMIP6' was used. NASA provided a csv file named 'gddp-cmip6-thredds-fileserver.csv' containing url files[4]. Using one url permitted to download the modelled climate variable of interest for a year, modelled with a certain model, under the condition of a certain experiment (SSPs and historical) and certain ensemble. Depending on the variable, ensemble, and years, a list of url files is selected. The function 'download_file' is then used to download the file. By modifying slightly the url, only the geographical zone around Mozambique was selected and downloaded, to save time and computer memory. To have a more rapid download of the files, a threadPool was applied, with the list of url files and the 'download_file' function.

Once the data of interest downloaded, for each climate variable, data were in several files of nc format. There was a need to gather the data by climate variable to compare the different values obtained with different models and experiments. Moreover, there was no need to have the data for the whole Mozambique.

Therefore, code 3 'CSV_NEX-GDDP-CMIP6_one_lat_lon' was then used to gather data for the projects of interest in a csv file. The function 'register_data_in_dataframe' opened the file of interest and found the closest data to the latitude and longitude of the project or the meteorological station. The final output was one csv with projection data per climate variable, during the period of interest. The code also produced two other csv files: one listing the name of the files that were corrupted, and the other listing the name of the files that did not exist.

To compare modelled data to observed data from NOAA station, there was a need to register modelled data close to the location of the NOAA station. This was done with code 4 'CSV_Obs_NEXGDDPCMIP6_one_lat_lon' which has the same structure as the precedent one. Only the coordinates of the location of interest are different.

2.3.4 Validation of data

A technical control was performed by NASA on the NEX-GDDP-CMIP6 set of data. For each climate variable, bounding values, a lower bound value and an upper bound value of the realistic range of the climate variable were set. The control process was to count how much values were out of the range of bounding values. Those values out of a realistic range are not necessarily mistakes However they should not occur often. Only 0.1% of the values were out of their corresponding range (39).

To check if the set of data is representative of the real world, observation data from NOAA were compared with modelled data at the same location (code 5). The report is looking into climate change at the location of the Gorongosa project; the closest meteorological station to this town is the one in Chimoio. Therefore. to see if modelized data are a good representation of reality for the Gorongosa project, modelized data which are the closest possible to the Chimoio meteorological station and the observed data from the Chimoio meteorological station are compared. Only the precipitation and temperature are compared.

Concerning observation temperature data from the NOAA dataset, some temperature values were around 99°C, whereas the hottest recorded temperature is 56.7°C (41). Data above 57°C were replaced by Nan values in the dataset. The code 6 permitted to treat those data

NEX-GDDP-CMIP6 daily air temperature modelled data follow a similar distribution to the one of the observed data in Chimoio, except for the models 'TaiESM1' and 'CMCC-CM2-SR5' (Figure 2-3 and Figure 0-1 in

[4] csv file coming from this technical note

Appendix B – Validation of NEX-GDDP-CMIP6 data). The average temperature of the dataset NEX-GDDP-CMIP6 can be kept to study the consequences of climate change on temperature in Mozambique, without the outputs of the outlier models. It is important to point out, that between 1970 and 2014, about 60 % observation average air temperature data are missing for the station of Chimoio (Figure 0-2 in Appendix B – Validation of NEX-GDDP-CMIP6 data). The comparison between observed and modelled data in the city of Beira are also added in the Appendix B – Validation of NEX-GDDP-CMIP6 data (Figure 0-3), to confirm that temperature modeled data are appropriate to use in Mozambique.

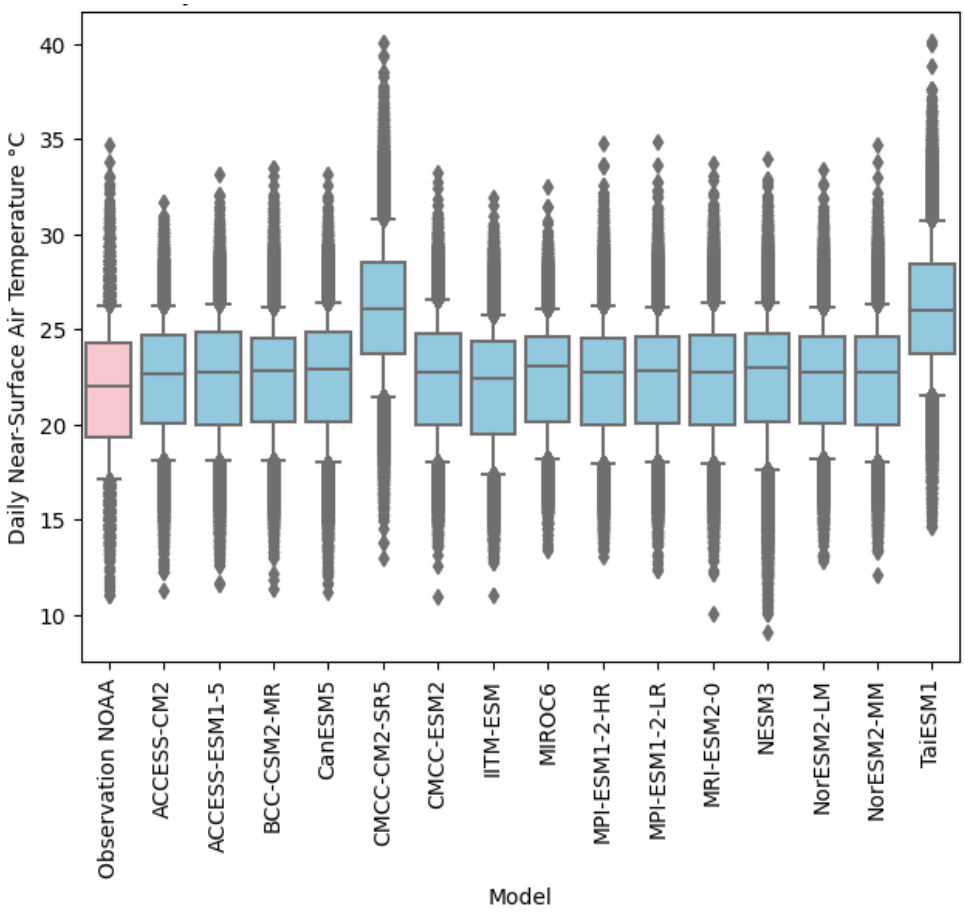

Figure 2-3 - Boxplots of the NEX-GDDP-CMIP6 modelled daily air temperature °C (in blue), compared to the boxplot of the daily air temperature °C registered by the meteorological station (in pink). Data are between 1970 and 2014 and are from Chimoio. The boxplots are presented with the median as the central line, the 25-th/75-th percentile as first and third quartile, the 10-th percentile and the 90-th percentile as whiskers and with outliers. Only the distribution of the models CMCC-CM2-SR5 and TaiESM1 do not comply with the observed distribution in pink.

Concerning the maximum air temperature, the modelled data have the same trends (Figure 2-4, Figure 2-6 and Figure 0-4). Between 1970 and 1990, the modelled average maximum temperature is always above the observed average (Figure 2-6). Modelled maximum air temperature data are higher over the whole distribution than the historic observations at Chimoio. Moreover, extreme modelled values are also higher than extreme modelled values (Figure 2-4 and Figure 0-4 in Appendix B – Validation of NEX-GDDP-CMIP6 data). Therefore, there is a bias between observed and modelled maximum air temperature data.

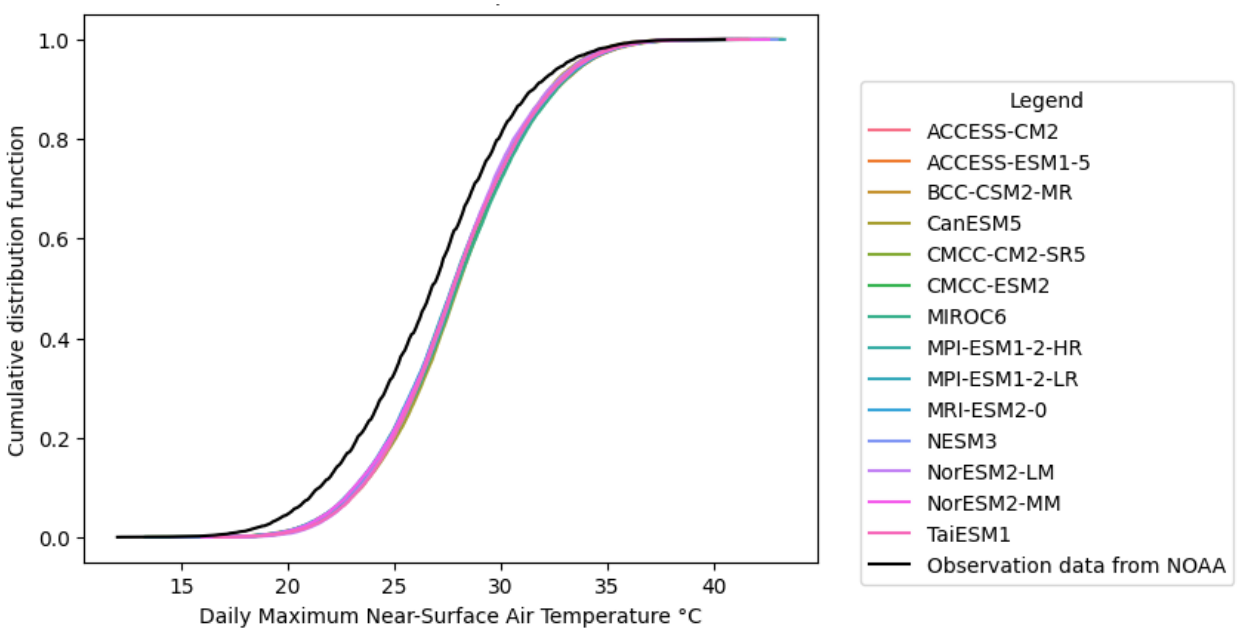

Figure 2-4 – Cumulative distribution functions (CDFs) of NEX-GDDP-CMIP6 modelled daily maximum air temperature °C, compared to CDF of observed maximum temperature data. All data are between 1970 and 2014 and are in Chimoio. Each colored line represents the CDF for the output data of a GCM. The black line is the CDF of the observed data at the meteorological station in Chimoio. All models are following the same distribution, which has higher values than the observed distribution.

As maximum air temperature modelled data, precipitation modelled data follow the same trends, but do not match all the trends of observed data (Figure 2-5, Figure 2-7, and Figure 2-9). Between 20 and 50 mm/day, modelled cumulative distribution functions (CDFs) are higher than observed CDF, meaning that modelled CDFs have smaller value than observed data (Figure 2-9). Moreover, observed data have some extreme daily values, that are never reached in modelized data (Figure 2-7 and Figure 2-9). Those observed extreme values are not mistakes; events from this magnitude are plausible in Mozambique (22). On the opposite, lower modelled and observed precipitation values follow the same trend and distribution without being similar (Figure 2-8). Looking at the modelled and observed average, their values are in the same range, between 800 and 1400 mm/year (Figure 2-5). In the end, precipitation modelled data in Chimoio are misleading for higher and extreme values.

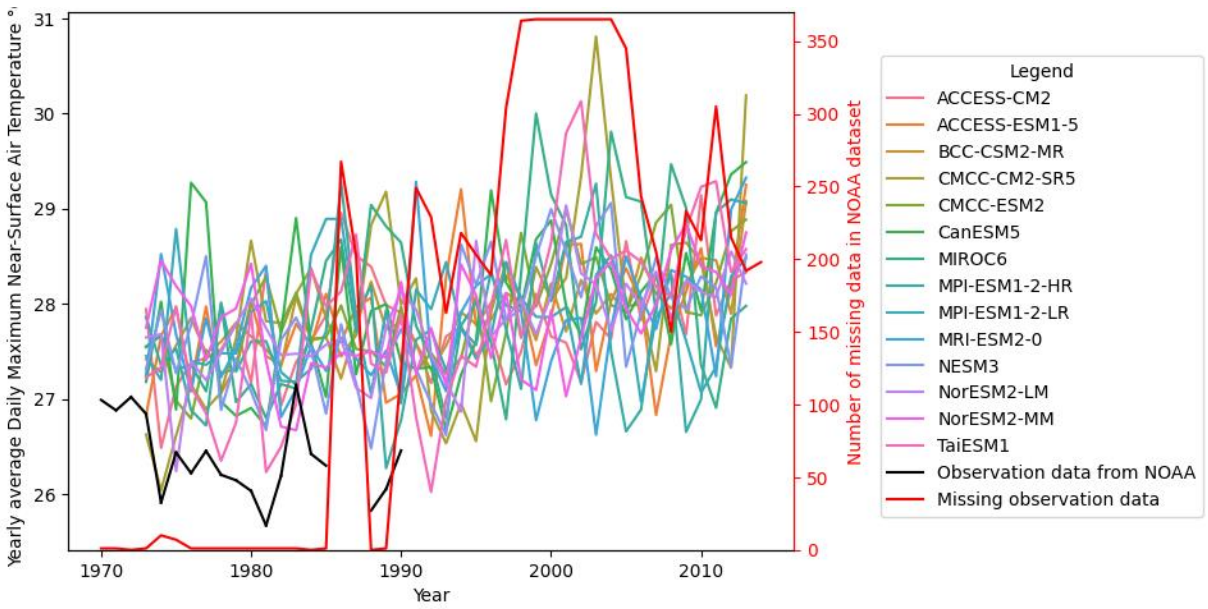

Figure 2-6 - Annual average maximum air temperature °C between 1970 and 2014 in Chimoio. Each colored line represents the output of one model, the black line represents the observed value. Those lines should be read with the left y-axis. The red line presents the number of missing data per year. It should be read with the right y-axis If a year is missing more than half of the observed value, the value of the observed data (black line) is not displayed. Between 1970 and 2014, 45% of the observed data are missing. Between 1970 and 1990, only 8% of observed data are missing. Between 1970 and 1990, the observed annual average is below all the modelled ones.

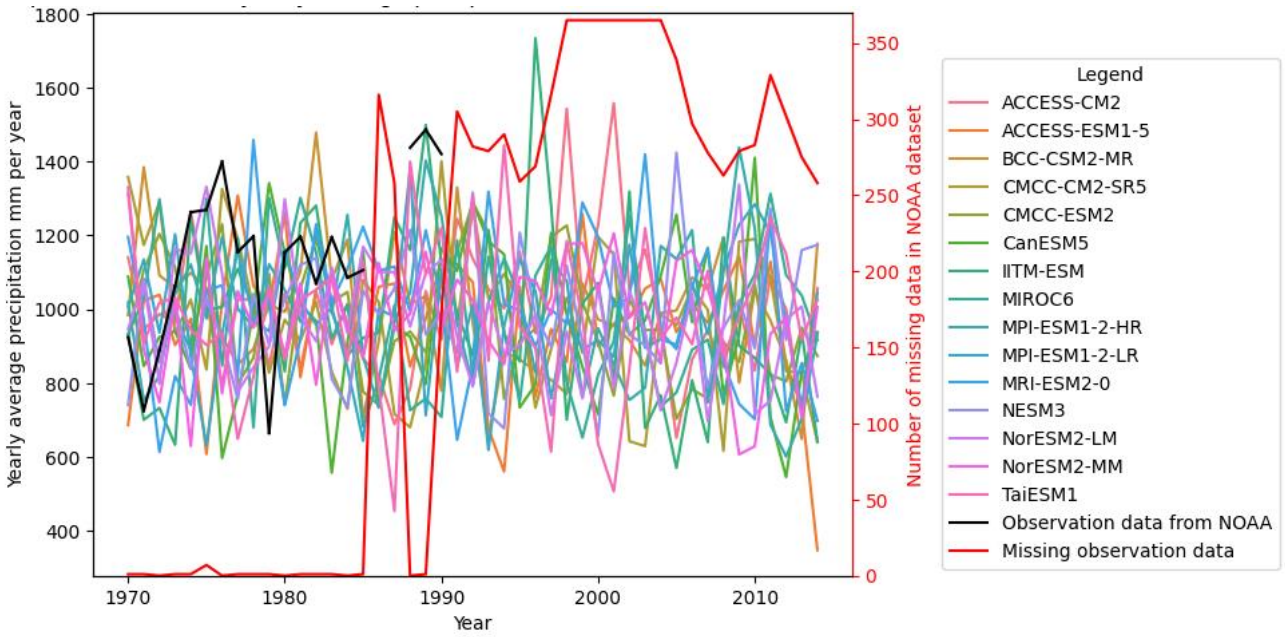

Figure 2-5 - Annual average precipitation mm/year between 1970 and 2014 in Chimoio. Each color line represents the output of one model, the black line represents the observed value. Those lines should be read with the left y-axis. The red line presents the number of missing data per year. It should be read with the right y-axis If a year is missing more than half of the observed value, the value of the observed data (black line) is not displayed. Between 1970 and 2014, 50% of the observed data are missing. Between 1970 and 1990, the annual average precipitation modeled concur with the observed one

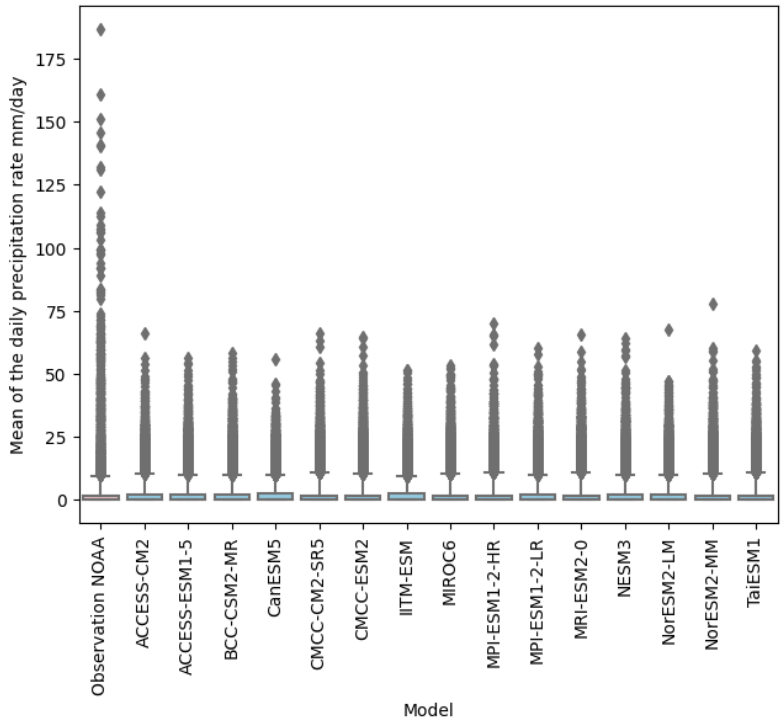

Figure 2-7 – Boxplots with outliers of the NEX-GDDP-CMIP6 modelled precipitation mm/day (in blue), compared to the one of the daily precipitation mm/day registered by the meteorological station (in pink, the first boxplot starting from the left). Data are between 1970 and 2014 and are from Chimoio. The boxplots are presented with the median as the central line, the 25-th/75-th percentile as first and third quartile, the 10-th percentile and the 90-th percentile as whiskers and with outliers. Extreme modelled precipitation data do not concur with extreme observed precipitation data.

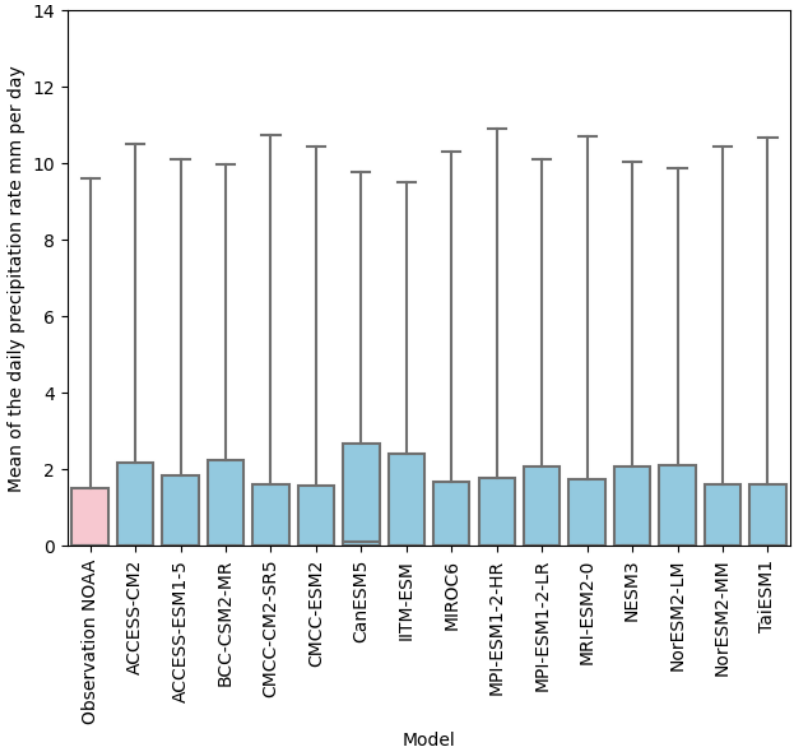

Figure 2-8 -Boxplots without outliers of the NEX-GDDP-CMIP6 modelled precipitation mm/day (in blue), compared to the daily precipitation mm/day registered by the meteorological station (in pink). Data are between 1970 and 2014 and are from Chimoio. The boxplots ar e presented with the median as the central line, the 25-th/75-th percentile as first and third quartile, the 10-th percentile and the 90-th percentile as whiskers and without outliers. The data concur on the third quartile and the 90-th percentile.

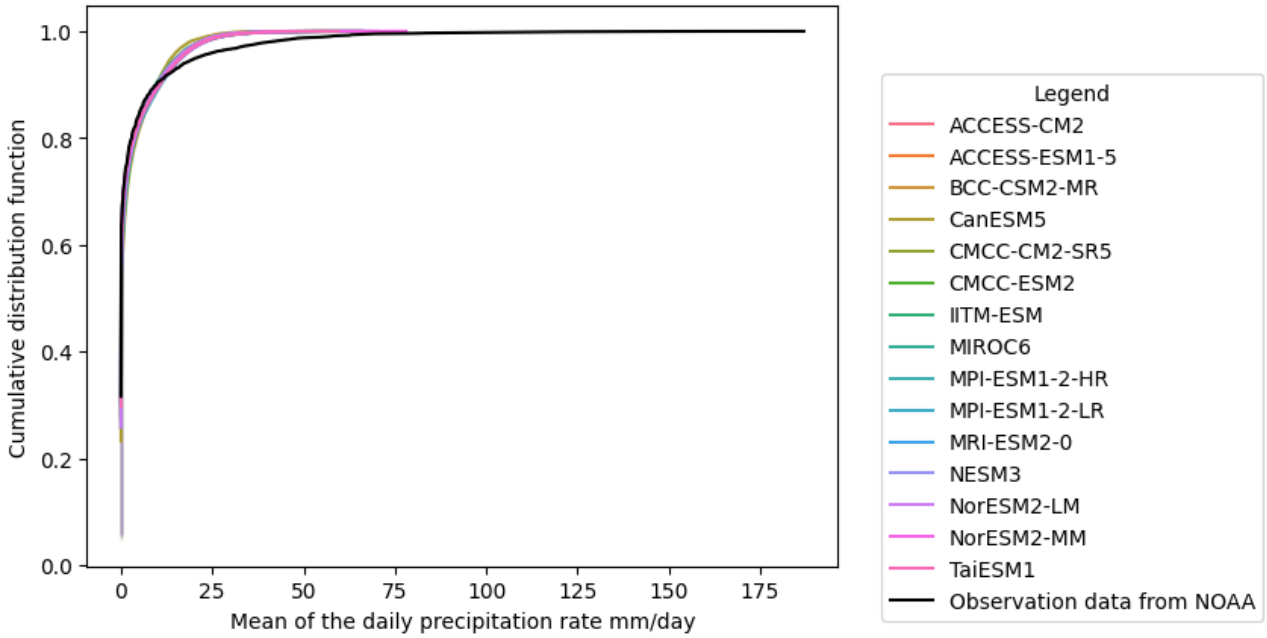

Figure 2-9 - CDFs of NEX-GDDP-CMIP6 modelled daily precipitation mm/day, compared to CDF of observed precipitation data mm/day . All data are between 1970 and 2014 and are in Chimoio. Each colored line represents the CDF for the output data of a GCM. The black line is the CDF of the observed data at the meteorological station in Chimoio. All models are following the same distribution, that does not comply with the observed distribution, particularly for the extremes.

Precipitation modelled data in Gorongosa present the same deficit as the ones in Chimoio concerning high and extreme values (Figure 0-5, Figure 0-6, Figure 0-7 in Appendix B – Validation of NEX-GDDP-CMIP6 data). Additionally, modelled values under the 75th percentile are higher than observed values under 75-th percentile (Figure 2-10). Therefore, modelled precipitation values in Gorongosa do not match any trend of observed values in Gorongosa.

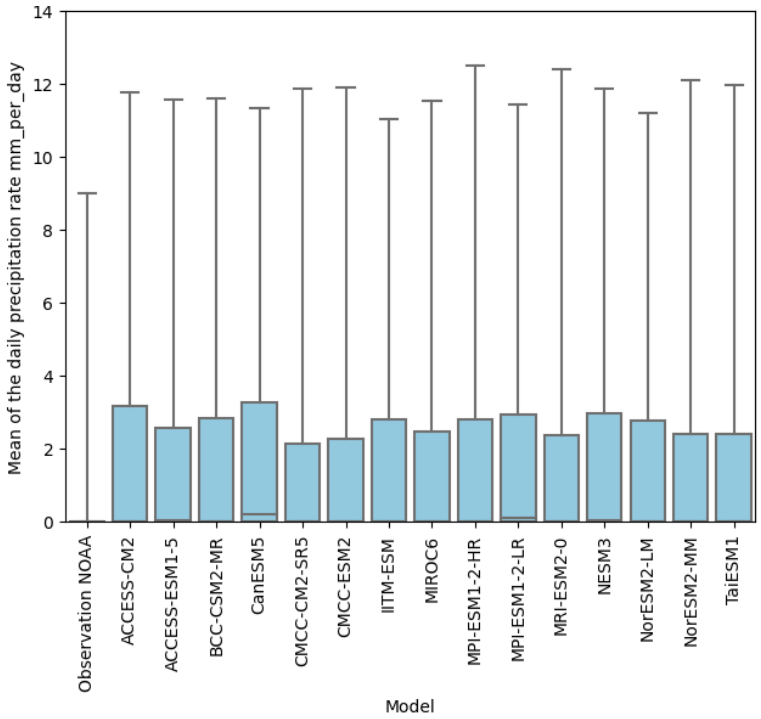

Figure 2-10 - Boxplots of the NEX-GDDP-CMIP6 modelled precipitation mm/day (in blue), compared to the boxplot of the precipitation mm/day registered by the meteorological station (in pink). Data are between 1980 and 2014 and are from Gorongosa. The boxplots are presented with the median as the central line, the 25-th/75-th percentile as first and third quartile, the 10-th percentile and the 90-th percentile as whiskers and with outliers. The observed third quartile is lower than the modelled one.

Outlier models CMCC-CM2-SR5 and TaiESM1 were removed for the following parts of this report. The model NESM3 was also taken out of the analysis because there was no available data for the scenario spp370. Maximum temperature and precipitation did not follow the distribution of the observed data. To correct those biases, bias correction can be used.

2.4 Bias correction

Bias correction (BC) is used to deal with the biases, differences between observed and modelled data induced in GCMS and RCMs (42,43). Those biases have three different sources: unrealistic large-scale response to climate forcings, unpredictable internal variability of the models different from the observed ones, and errors in parametrization and unresolved subgrid-scales in mountains. Theoretically, BC mostly permits to correct the third source (44). According to (Wu 2022) (27), BC also permits to reduce uncertainty in projections. BC methods have two categories: scaling-based technics and distribution-based technics (45)[5](46). The first category encompasses technics adjusting climate models outputs with linear or nonlinear formulas. Distribution base technics correct climate model outputs with distribution functions fitted on observation and modelled data (46). Quantile mapping (QM) is part of the distribution-based technics (45).

2.4.1 Quantile mapping method

QM is one of the most popular methods (44,47) for two reasons. The method outperforms simpler methods (27,43,44,48), such as linear scaling or variance scaling (49). Additionally, the method is computationally efficient (47). QM consist of two steps:

[5] GitHub - ElsevierSoftwareX/SOFTX-D-23-00031: Bias correction command-line tool for climatic research written in C++

1. Define two cumulative distribution functions: one with the modeled data from the past, and one with observation data (Image on the right side of Figure 2-11). Data chosen should be for the same period (44).
2. Apply the transform of those 2 CDFs (Equation 1) on each value to correct in the set of projection data (arrow in the image on the right side of Figure 2-11). This will give the bias corrected projected value (44).

$$\hat{x}_{m,p}(t) = F_{o,h}^{-1}\{F_{m,h}[x_{m,p}(t)]\}$$ Equation 1 - Transfer function used in Quantile mapping (44)

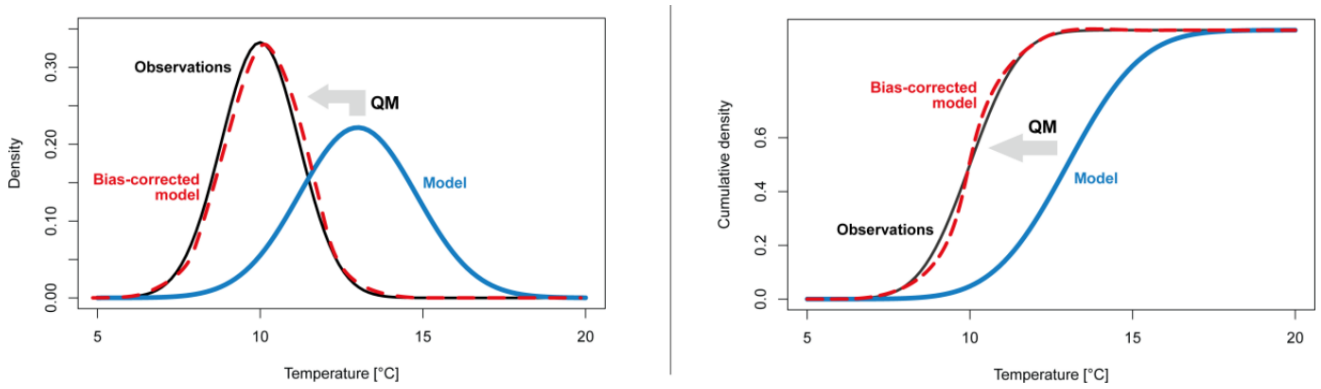

Figure 3: The nature of QM: A biased simulated distribution (blue) is corrected towards an observed distribution (black). In the example shown the raw simulated distribution is subject to both a bias of the mean and a bias in variance. The resulting bias-corrected distribution (dashed red) approximates the observed one but is typically not identical to it (e.g. due to the sampling uncertainty during the calibration of the correction function or details of the specific QM implementation). Left panel: Example based on the probability density function (PDF). Right panel: example based on the cumulative distribution function (CDF).

Figure 2-11 -Figure 3 from 'Exploring quantile mapping as a tool to produce user-tailored climate sceanrios for Switzerland' (50), presenting functioning from quantile mapping

Bias corrected value for a certain model m in a projected period of time (denoted by the subscript p) $\hat{x}_{m,p}(t)$, is obtained with the inverse CDF $F_{o,h}^{-1}$, determined with observed data o in the past h, and the CDF $F_{m,h}$, determined for model m in the past h, with as input $x_{m,p}(t)$ a modeled value at time t within some projected periods p.

QM can be based on an empirical distribution (non-parametric distribution) or a fitted theoretical distribution (parametric distribution) (50). According to (44), QM that rely on non-parametric distribution outperforms those that fit a parametric distribution to data.

All BC methods perform on a calendar basis: statistic properties for a certain period (month or season) between modelled and observed data are equalized (42).

QM application relies on two main assumptions. The first is that the rank of GCM data is correct and can be used to produce a CDF. But not the actual magnitude of the values is wrong and should be corrected (50). The second is stationarity: characteristic in the historical period will persist in the future (44). Validity of this assumption will be discussed in section 3.2 Discussion of bias correction results.

2.4.2 Bias Correction Spatial Disaggregation - BCSD

Another bias correction method is Bias Correction Spatial Disaggregation (BCSD). It is performed in 2 steps: bias correction, followed by downscaling (51).

Principle of bias correction are explained in 2.4 Bias correction. Concerning the second step, downscaling the dataset permits to have a dataset with a lower resolution. Future trends can be analyzed in a more localized way (25,52). 2 different types of downscaling exist; statistical downscaling (GCMs linked to observation data with statistical models), and dynamical downscaling (one or several RDMs is run over a limited region, with coarse GCMs as boundaries and initial data). Dynamical downscaling is very computational demanding and statistical downscaling is much more straightforward (52). The methods can be applied in a complementary way for one dataset (52). To downscaled CMIP6 data, NEX-GDDP-CMIP6 used statistical downscaling. Downscaling is also called spatial disaggregation (39).

According to (Wu 2022) (27), in comparison to other simpler methods (delta change, QM and nonstationary cumulative-distribution function-matching), BCSD perform better to reduce uncertainty of projections.

2.4.3 Implementation of Bias Correction

BCSD was implemented by NASA to bias correct certain NEX-GDDP-CMIP6 climate variables. Those bias corrected data were bias corrected a second time. The code used to perform this second BC is explained below.

A package named scikit-downscale contains a lot of possibilities to perform bias correction (53)[6]. This tool is meant to perform statistical downscaling using Scikit-learn (54), which is python module for machine learning built on top of SciPy (55,56). The GitHub of the package was cloned on the GitHub of this project, to add the functions needed to perform BC.

With scikit-downscale, the user can choose between several models to BC. For this report, BcsdTemperature and BcsdPrecipitation were used to BC respectively, maximum temperature and precipitation data. Those methods are based on the BCSD method (51), explained in 2.4.2. In the function of scikit-downscale, only QM is applied. The method is applied monthly, which means that data for every month are mapped to perform QM.

Concretely, BcsdTemperature and BcsdPrecipitation were used with the input 'return_anoms=False', to have the bias corrected data and not the climatic anomalies as output. For each model the same procedure is applied:

- The user must define a set of data among the modelled data and the observed data (respectively X_pcp and y_pcp in the figure below) within a certain period to fit the model, and another set of data among the modelled data in another period to be corrected (X_correct in the Figure 2-12). The fitted period and the predicted period should not overlap
- The model chosen is then fitted with the set of data to fit (second line in the Figure 2-12)
- The bias corrected data are obtained using the predict function with the data to correct as input (third line in the Figure 2-12)

```
bcsd_temp = BcsdPrecipitation(return_anoms=False)
bcsd_temp.fit(X_pcp, y_pcp)
out = bcsd_temp.predict(X_to_correct)
```

Figure 2-12 - Basic implementation of BC with Python

BC for NEX-GDDP-CMIP6 was performed with code 7.

[6] Scikit-downscale Github

- The user choses the wanted climate variable to correct, and the wanted years to correct
- The code imports packages and functions
- Before the BC is applied, some models are removed because for some climate variables, they were not representative of the reality, and others did not have data for every scenario
- The BC is applied for each location, scenario and model. Depending on which climate variable was corrected, the function BCSD_Precipitation_return_anoms_to_apply is applied for precipitation and the function BCSD_Temperature_return_anoms_to_apply is applied for maximum temperature. Those 2 functions applied the content in Figure 2-12 and were defined in code 8 Bias_correction_function. Those 3 for loops permit to correct data for each project, each scenario and model separately.

2.5 Methodology of climate risk and vulnerability analysis

Since a few years, EU promotes climate adaptation strategies (14)(16). Regarding this objective, guidelines were written to help project managers of physical assets and infrastructures to take into account and adapt their project to climate variability and future climate change (16). This method allows to estimate the risks for a project regarding certain climate variables, and then integrate the attenuation implemented to investigate the residual risks.

To identify which elements of a project is submitted to climate risk, analysis should be performed on the four key project themes cited next:

- On-site assets and processes: elements of infrastructure that compose physically the project or that occur/work on site (example: pumps and treatment processes in a WTP)
- Inputs: elements introduce in the infrastructure to make it operate it (example: chemical inputs for the flocculation process in a WTP)
- Outputs: elements coming out of an infrastructure (example: water for a WTP)
- Transport links: means of transport on which the project is dependent (example: roads to bring chemical inputs for WTP)

The method to apply is composed of the following steps (15) (16) (14):

1) Choice of climate variable changes to evaluate
2) Vulnerability assessment
3) Risk assessment
4) Climate adaptation

The list climate variable to be assessed will drive the final outcomes. Ideally, all climate variable changes having a major influence on climate should be assessed. Indicators are meant to be more precise in the impact to be assessed and to represent the climate variable or the second effect variable. Their aim is to permit to monitor the influence of climate change on the climate variable (example: value of 100-year return period event)

Vulnerability assessment: vulnerability is the circumstances/characteristics under which an element of the infrastructure can be affected by a hazard (definition of a hazard: a potentially damaging physical event, phenomenon or human activity that may cause the loss of life or injury, property damage, social and economic disruption, or environmental degradation (16). The assessment allows to know the degree of vulnerability of an element of a project to a certain climate variable, to which the element of the project is sensitive and to which the location of the project is exposed. Therefore, this step crosses the levels of sensitivity and of exposure, as shown in the matrix in Table 2-3.

Sensitivity is the degree by which an element of the infrastructure is affected, in a positive or negative way, in a direct or in an indirect way, by the variations of climate or climate change. The sensitivities to the chosen

climate variables of the assets, inputs, outputs, and interdependencies of the project are evaluated from high to no sensitivity. If data are available, they can be used. But if there is none, the evaluation will be based on expert judgement. This step only depends on the type of infrastructure proposed in the project.

Exposure is the degree to which the location of the project can be affected by climate change. Based on the magnitude of change of each indicator and its uncertainty at the location of the project, a level of exposure can be assigned (High to no exposure) for each project's element under each climate variable. Exposure only depends on the location of the project. In this step, the lifetime of the infrastructure determines which horizon is used for climate analysis. As projections are estimated with several models, and it has not been established which model was better than the other, uncertainty was evaluated across several models. The exposure is determined as follow

- if no significant or extreme changes are expected, exposure is low
- if a least one of the indicators of a climate variable goes under significant change (between +/- 20% or 50 %) with high uncertainty (10^{th} and 90^{th} percentile), exposure is medium
- if a least one of the indicators of a climate variable goes under extreme change (more than +/-50 %) with high uncertainty (10^{th} and 90^{th} percentile) or if a least one of the indicators goes under significant changes (between +/- 20% or 50 %) with low uncertainty (median), exposure is high

Table 2-3 -Vulnerability matrix, crossing sensitivity and exposure information

Vulnerability	**Exposure**		
Sensitivity	**No**	**Medium**	**High**
No	No	No	Medium
Medium	No	Medium	High
High	Medium	High	High

Risk assessment: in this method, risk is the product of severity of an event on a vulnerable element of the project, and likelihood of the same event, as shown in Table 2-4. Events are indicators of the climate variable (Example: for maximum temperature, an event could be the temperature going beyond 40 °C). Risk assessment will only be applied on elements of the infrastructure that have at least a medium level of vulnerability under some climate variables.

Severity measures the consequences (economic impact, structural damage, interruption of service) of an event on an element of the infrastructure. For each climate variable to which an element of the infrastructure is vulnerable, the impact of a certain event of this climate variable on the element of the infrastructure must be assessed based on data or expert judgement.

Likelihood is the probability of the event for a certain climate variable and can be set up with the projections data. Depending on the event, the likelihood can be only determined with the climate variable data. The final output of the likelihood depends on the quantitative value of the event's likelihood, as shown in Figure 2-13. Having several climate models, the probability was calculated within each of the models, for each SSPs. The final probability was the mean of all probabilities, across each model and SSP.

Quantitative (*)	Term
5 %	Rare
20 %	Unlikely
50 %	Moderate
80 %	Likely
95 %	Almost certain

Figure 2-13 - Classification term for probability likelihood (57)

Table 2-4 - Risk matrix, crossing severity and probability information, with the scale of risk associated

	Probability	Rare	Unlikely	Probable	Likely	Almost Certain
Severity		1	2	3	4	5
Insignificant	1					
Minor	2					
Moderate	3					
Major	4					
Catastrophic	5					

Scale of risk	1	2	3	4	5
	Rare	Unlikely	Possible	Likely	Almost Certain
Meaning:	Highly unlikely to occur	Given current practices and procedures, this incident is unlikely to occur	Incident has occurred in a similar country / setting	Incident is likely to occur	Incident is very likely to occur, possibly several times

Climate adaptation: is the step where some adjustments on the project's elements are implemented to cope with risks due to climate change or variability. Those adjustments will reduce impacts of the event on the project's elements. Knowing the climate variables under which the project's elements present the highest risks, the following steps are applied for climate adaptation:

a. Identification of adaptation/mitigation measures for each element of the project submitted to a risk
b. Integration of adaptation measure in project regarding management and technic
c. Residual risk calculation: return to step 3 (Risk assessment) and adapt severity level to the new adaptation measure in the project's element
d. Monitoring of the project: during the lifetime of the project, check that events to which project's elements are submitted to a risk do not exceed alarming thresholds, which are fixed after the implantation of the climate adaptations.

Guidelines can be applied to 'Climate-influenced projects' and to 'Climate adaptation projects'. First category includes projects which may fail if climate change is ignored, and second category are projects designed to reduce vulnerability due to climate hazards (16).

This method was not designed to take over the design of projects. The aim is for decision maker to see if their project is resilient against climate change and improve risk management of projects (16).

In this report, the focus will be mainly on the vulnerability step.

The methodology is applied in the code 1 CRVA_data_analyst. All the function in the Table 2-5 are called in this code.

Table 2-5 - Functions used in the code to implement steps of the CRVA

Step	Corresponding functions
Sensitivity	function 'sensitivity' (in code 9 Functions_ImportData) with no inputs. This function returns the dataframe containing the information given by the user in a csv format. The function has a pre-determined path that the user should change if the sensitivity path or file changed.
Exposure	1. function 'df_stat_distr' (in code 10 Functions_Indicators) calculates the statistical distribution of the data (count, mean, standard deviation, minimum, 10th percentile, median, 90th percentile and maximum) for each indicator. It should be calculated for a period in the past and another in the future (function 'filter_dataframe' in code 10 Functions_Indicators can be used to select periods, models and projects efficiently) 2. To know the relative change between past and future, the function 'changes_in_indicators' (in code 10 Functions_Indicators) was applied with the past and future statistical distribution as inputs for each indicator 3. function 'level_exposure' (in code 10 Functions_Indicators) gives the level of exposure at the location of the project for each climate variable, based on the relative change of the indicators, calculated with the function in precedent step
Vulnerability	In the CRVA_data_analyst code, the function 'vulnerability' (in code 9 Functions_Indicators) take as input the sensitivity dataframe and the exposure dataframe to have the vulnerability matrix.
Likelihood	'likelihood_accross_models_and_ssps' (in code 1 Functions_likelihood) gives the value of the average probability of an event across all SSPs and models, and the term associated to the value following Figure 2-13.

Several indicators were implemented in this code. They are listed in Table 2-6.

Table 2-6 - Functions to implemented indicators in the code

Climate variables changes	Indicators	Code to obtain the indicator
Incremental air temperature change	Average temperature per year	With the ' Daily Near-Surface Air Temperature °C' (tas), for each scenario and for each model, the average temperature per year is calculated with the function 'temporal_avg' in code 10 Functions_Indicators.
Extreme air temperature increase	Maximum temperature in year	With the 'Daily Maximum Near-Surface Air Temperature °C' (tasmax), apply function 'temporal_max' from code 10 Functions_Indicators .
	Daily maximum temperature	use the 'Daily Maximum Near-Surface Air Temperature °C' (tasmax)
	Annual number of days with temperature above a certain threshold temperature	With the 'Daily Maximum Near-Surface Air Temperature °C' (tasmax), apply 'number_day_above_threshold' from code 10 Functions_Indicators
Incremental rainfall change	Average yearly precipitation	With the precipitation data, used the function 'temporal_avg' with temporal_resolution (fourth input) as 'year' (in code 10 Functions_Indicators). This gave the average yearly precipitation for each SSP and model
	Average monthly dry or wet season precipitation	With the precipitation data corresponding to the dry or wet season, used the function 'temporal_avg' with temporal_resolution (fourth input) as 'month' (in code 10 Functions_Indicators). This gave the average monthly precipitation for each SSP and model. The wet season goes from October to March (12)
Extreme rainfall change	Maximum one day rainfall	With the precipitation data, used the function 'temporal_max' (code 10 Functions_Indicators). Depending on if the user wants the maximum one-day rainfall per month or per year, the fourth input of the function should, respectively, be 'month' or 'year'. The result will be the maximum value of precipitation per month or per year, for each SSP and each model. The user can also use the 'dataframe_1_day_event' (code 10 Functions_Indicators); the result will be the maximum value of precipitation per year, for each SSP and each model.
	Maximum five days rainfall	With the precipitation data, 'dataframe_max_5_days_event' in code 10 Functions_Indicators
	Event with 100 year return period	With the precipitation data, function 'dataframe_threshold_coresponding_to_return_period_model' in code 10 Functions_Indicators. The right-skewed gumbel distribution was chosen for the probability distribution function of the precipitation data (58). The extreme values were selected with the Annual Maxima method (59)
	Future return period of one day rainfall event with a current return of 100 years	With the precipitation data, 'dataframe_return_period_coresponding_to_past_100year_event_model' but the results are not as excepted. This function should be bettered (code 10 Functions_Indicators)

3 Results and discussion

3.1 Bias correction

Bias correction was applied for maximum temperature and for precipitation (respectively with BcsdTemperature and BcsdPrecipitation methods). The modelled data used were NEX-GDDP-CMIP6 data close to the meteorological station in Chimoio. The observed data used were from Chimoio. The bias correction was fitted over the period 1970-1984 and was applied over the period 1985-2014.

3.1.1 Maximum temperature

Trends in bias-corrected modelled maximum air temperature distributions are much closer to observed trend than non-bias-corrected modelled maximum air temperature distributions (respectively Figure 3-3 compared to Figure 3-1, and Figure 3-4 compared to Figure 3-2). Extreme values, small and high, still do not comply completely with observed ones. The minimum value reached was around 7 °C with the model 'CanESM5'. For the observed data, it was around 12 °C. The maximum value reached was around 45 °C with the model 'CMCC-ESM2'. For the observed data, it was around 39 °C (Figure 3-4).

The attention should be raised to the fact that, about 60 % of the observed maximum temperature data between 1984 to 2014 are missing (Figure 2-4). Concerning the data used for the fitting of the model of bias-correction, only 0.2 % of the data were missing in the period 1970-1984.

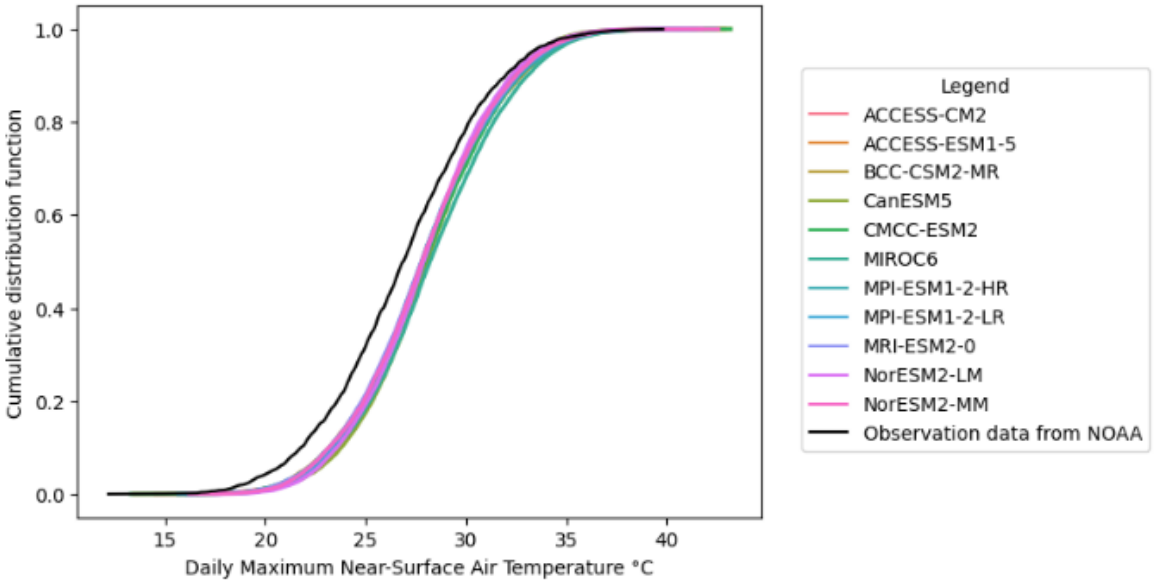

Figure 3-1- CDFs of NEX-GDDP-CMIP6 modelled daily maximum air temperature °C not bias-corrected, compared to observed average temperature from the Chimoio meteorological station between 1985 and 2013. Each colored line represents the CDF for the output data of a GCM. The black line is the CDF of the observed data at the meteorological station in Chimoio. All models are following the same distribution, which has higher values than the observed distribution.

The bias-corrected maximum air temperature distributions comply better to observed ones than non-bias-corrected ones, but extreme values are still not completely representative of reality.

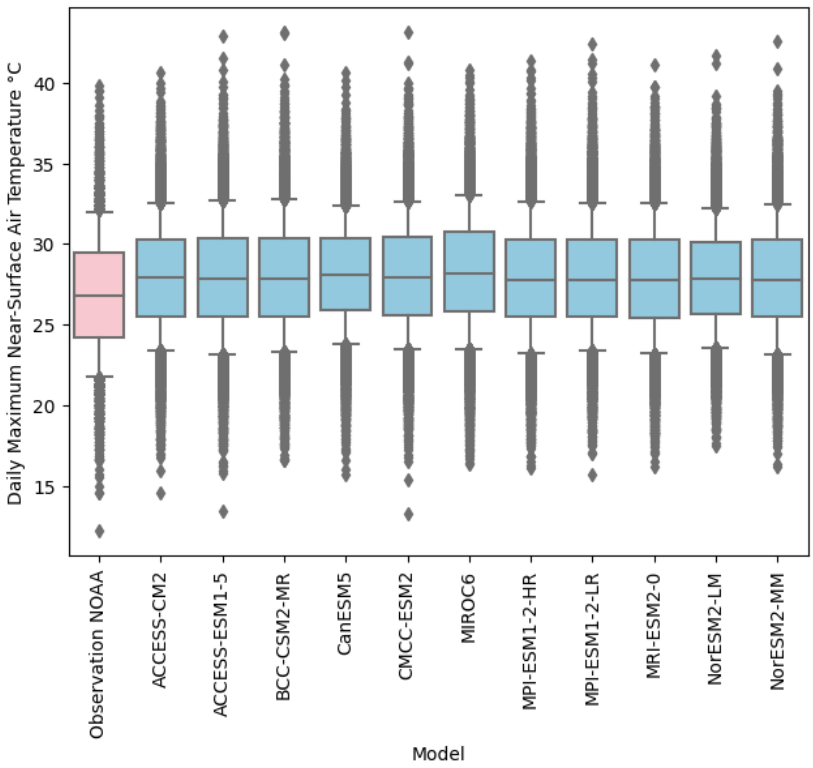

Figure 3-2 - Boxplots of the NEX-GDDP-CMIP6 modelled daily maximum air temperature °C (in blue) not bias corrected, compared to the boxplot of the daily maximum air temperature °C registered by the meteorological station (in pink). Data are between 1985 and 2013 and are from Chimoio. The boxplots are presented with the median as the central line, the 25-th/75-th percentile as first and third quartile, the 10-th percentile and the 90-th percentile as whiskers and with outliers. Modelled distributions are slightly higher than observed data

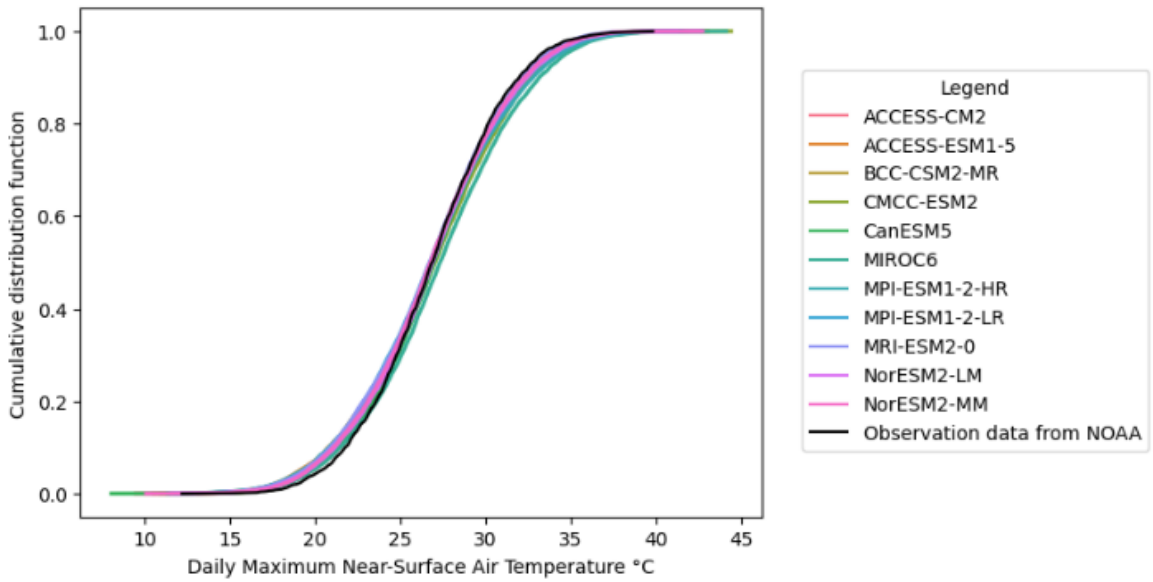

Figure 3-3 - CDFs of NEX-GDDP-CMIP6 modelled daily maximum air temperature °C bias-corrected, compared to CDF of observed maximum temperature data. All data are between 1985 and 2013 and are in Chimoio. Each colored line represents the CDF for the output data of a GCM. The black line is the CDF of the observed data at the meteorological station in Chimoio. Modelled distributions all follow the observed one.

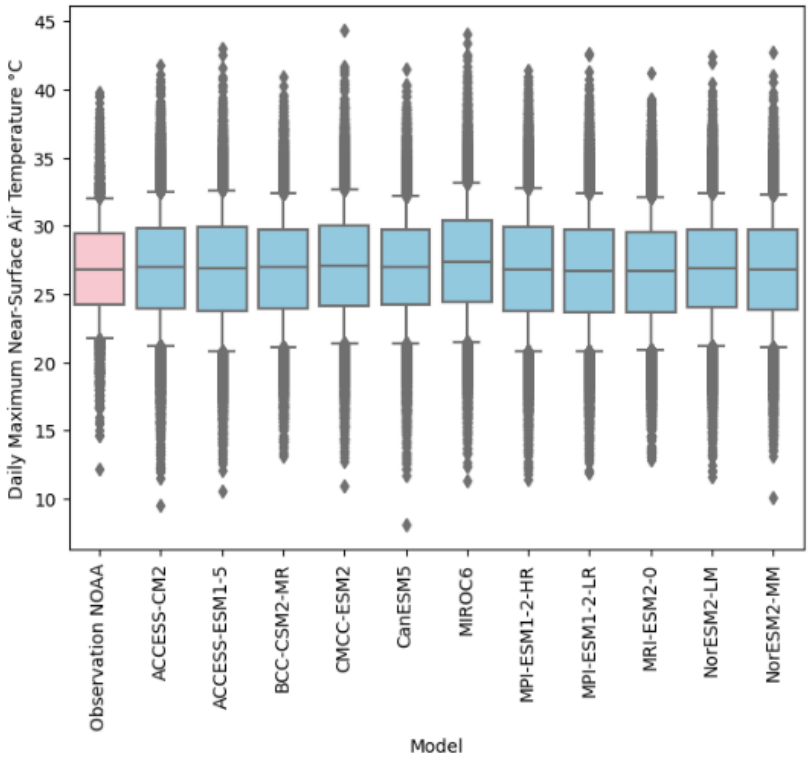

Figure 3-4 - Boxplots of the NEX-GDDP-CMIP6 modelled daily maximum air temperature °C (in blue) bias corrected, compared to the boxplot of the daily maximum air temperature °C registered by the meteorological station (in pink). Data are between 1985 and 2013 and are from Chimoio. The boxplots are presented with the median as the central line, the 25-th/75-th percentile as first and third quartile, the 10-th percentile and the 90-th percentile as whiskers and with outliers. Modelled distributions are closer to the observed distribution than in Figure 3-2

3.1.2 Precipitation

The CDFs of the models are closer to the observed CDF than before non-bias-corrected data (respectively Figure 3-6 compared to Figure 3-5). However, the distribution of data under 30 mm per day do not overlay the distribution of modelled ones except for the extreme minimums; the modelled data are slightly to the left of the observed CDF (Figure 3-6). Moreover, outliers and 90th percentiles of the modelled data were all lower than the ones of the observed data (Figure 3-8). Therefore, the global distributions of precipitation bias-corrected data are closer than the non-bias-corrected ones, but bias-corrected modelled data are lower values than observation data.

Outliers of the modelled distributions are similar from one model to another in the bias-corrected data (Figure 3-8). The 90th percentile have the same value for every model; the third quartile (75th percentile) do not vary from one model to the other (Figure 3-10). It is not possible to talk about the median and 25th percentile, as they cannot be seen on the figures.

The extremes of bias-corrected data do not comply with the observed ones (Figure 3-6). The maximum value for observed data is around 177 mm per day, the maximum value for the modelled data is around 160 mm per day (Figure 3-8).

As for maximum temperature, the attention should be raised on the fact that, as it can be seen with Figure 2-5, about 75 % of the observed precipitation data between 1985 to 2014 are missing. Concerning the observed data used to fit the model, there was almost no data missing for the fitting period used.

Bias-corrected precipitation data have higher extremes closer to observed ones than non-bias-corrected values. However, those extremes are all similar. Moreover, lower values distributions of bias-corrected precipitation data do not comply with lower values distributions of observed data.

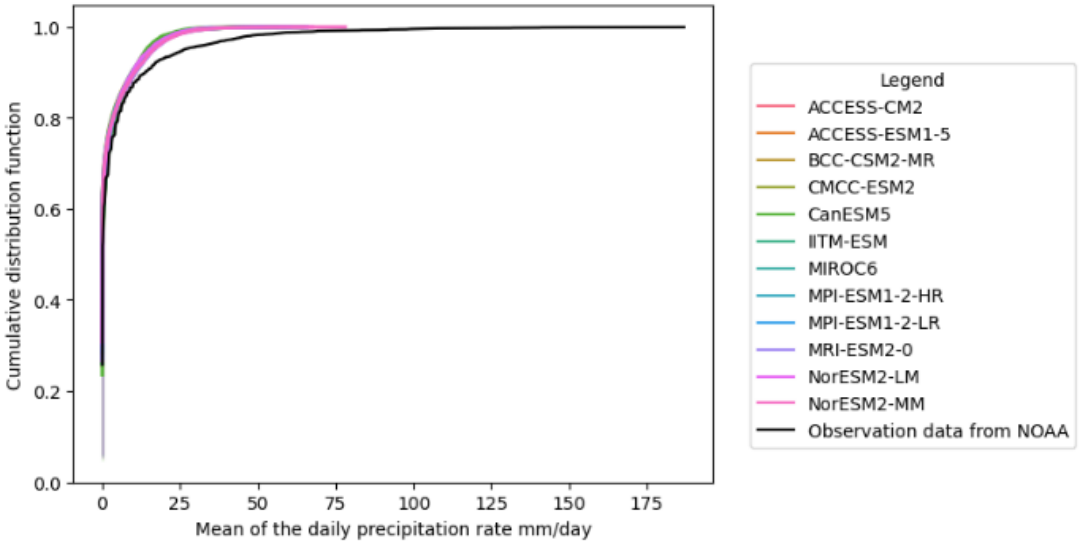

Figure 3-5 - CDFs of NEX-GDDP-CMIP6 modelled daily precipitation mm/day not bias-corrected, compared to CDF of observed precipitation mm/day data. All data are between 1985 and 2014 and are in Chimoio. Each colored line represents the CDF for the output data of a GCM. The black line is the CDF of the observed data at the meteorological station in Chimoio. Modelled data have smaller values. Moreover, extremes modelled values are much smaller than observed ones.

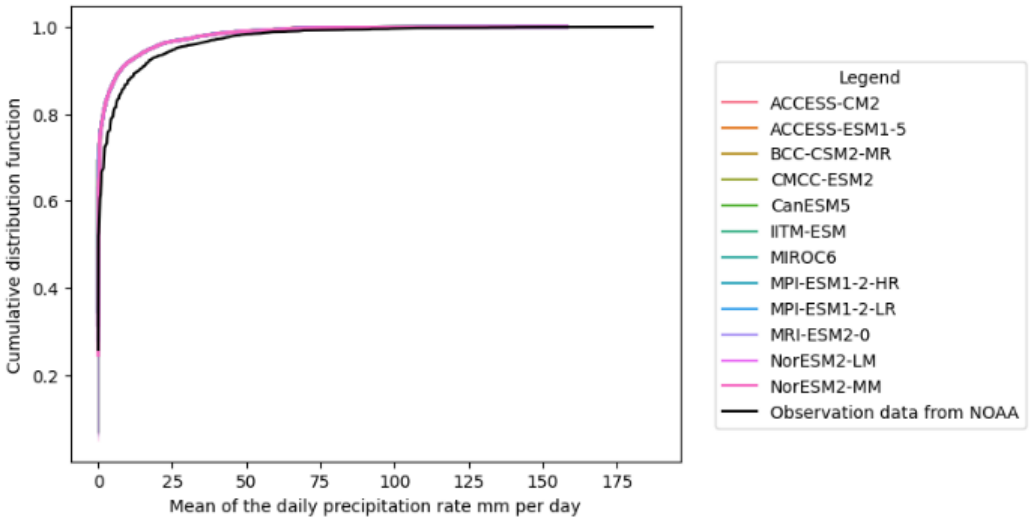

Figure 3-6 - CDFs of NEX-GDDP-CMIP6 modelled daily precipitation mm/day bias-corrected, compared to CDF of observed precipitation mm/day data. All data are between 1985 and 2014 and are in Chimoio. Each colored line represents the CDF for the output data of a GCM. The black line is the CDF of the observed data at the meteorological station in Chimoio. Bias-corrected modelled data still have smaller values. But bias-corrected extremes modelled values are closer to observed ones.

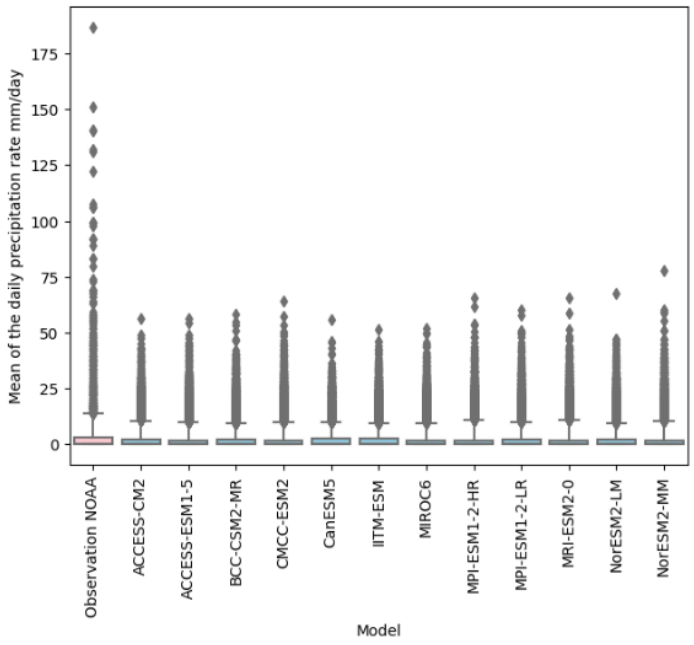

Figure 3-7 - Boxplots of the NEX-GDDP-CMIP6 precipitation mm/day (in blue) not bias corrected, compared to the boxplot of the precipitation mm/day registered by the meteorological station (in pink). Data are between 1985 and 2014 and are from Chimoio. The boxplots are presented with the median as the central line, the 25-th/75-th percentile as first and third quartile, the 10-th percentile and the 90-th percentile as whiskers and with outliers. Modelled extremes are much lower than observed ones.

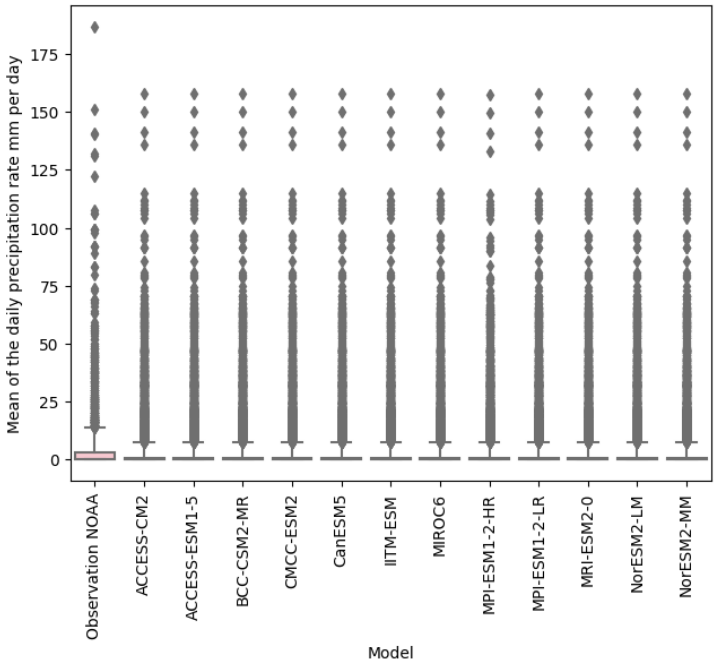

Figure 3-8 - Boxplots of the NEX-GDDP-CMIP6 precipitation mm/day (in blue) bias corrected, compared to the boxplot of the precipitation mm/day registered by the meteorological station (in pink). Data are between 1985 and 2014 and are from Chimoio. The boxplots are presented with the median as the central line, the 25-th/75-th percentile as first and third quartile, the 10-th percentile and the 90-th percentile as whiskers and with outliers. Modelled extremes are closer to the observed ones than in Figure 3-7. But they all follow the same distribution.

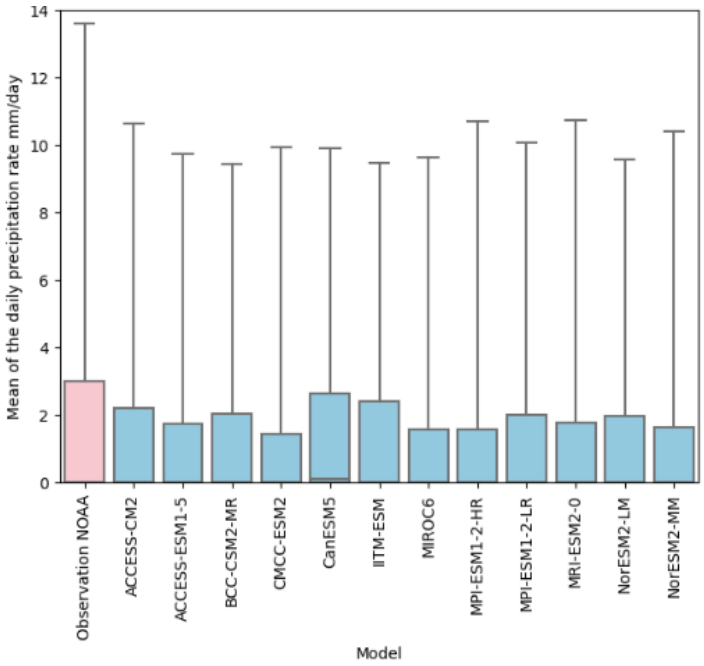

Figure 3-9 - Boxplots without outliers of the NEX-GDDP-CMIP6 precipitation mm/day (in blue) not bias corrected, compared to the boxplot of the precipitation mm/day registered by the meteorological station (in pink). Data are between 1985 and 2014 and are from Chimoio. The boxplots are presented with the median as the central line, the 25-th/75-th percentile as first and third quartile, the 10-th percentile and the 90-th percentile as whiskers and without outliers. 90-th percentile of observed distribution is higher than the ones of modelled distribution. The observed and modelled quartiles are closer.

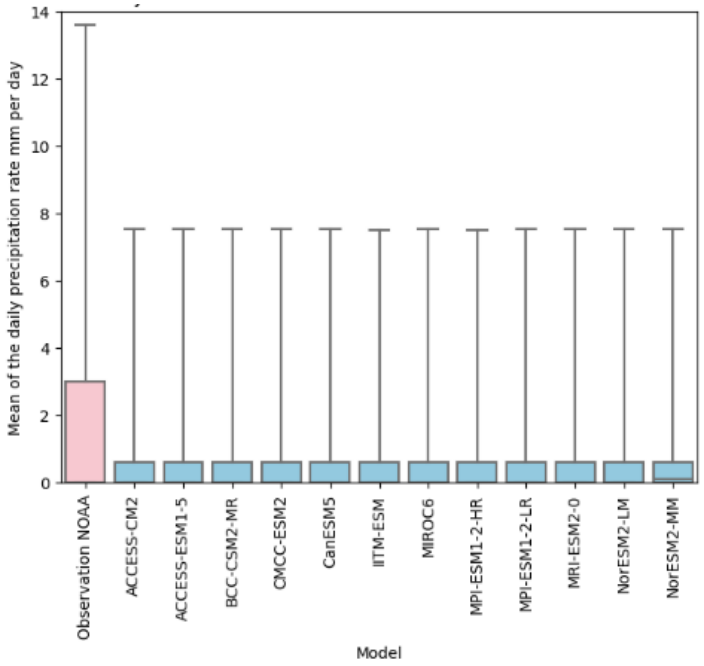

Figure 3-10 - Boxplots without outliers of the NEX-GDDP-CMIP6 precipitation mm/day (in blue) bias corrected, compared to the boxplot of the precipitation mm/day registered by the meteorological station (in pink). Data are between 1985 and 2014 and are from Chimoio. The boxplots are presented with the median as the central line, the 25-th/75-th percentile as first and third quartile, the 10-th percentile and the 90-th percentile as whiskers and without outliers. 90-th percentile between modelled data have the same value and are much lower the observed one.

3.2 Discussion of bias correction results

Concerning BC on maximum temperatures, the distribution of results did not perfectly match the observed distribution for the extremes values. But the median, first and third quartiles, 10-th and 90-th percentile comply with the behavior of the observed distribution, without having the same behavior for every model. This was not the case for precipitation, where the results of BC were all similar for extremes between models.

In the scikit-downscale package, BC is performed based on a non-parametric estimation for quantiles. However, some studies indicated that to apply QM on precipitation (42–44), the functions used to compose the transform function for mapping are gamma distribution functions fitted on observed and modelled data. The choice of the gamma probability distribution is often made for BC of precipitation because of the wide variety of distribution shape that can be obtained with the gamma distribution (42). Other distribution functions can be applied, like in this study for the BC of precipitation in South Korea (43), where the Kappa distribution function is considered to represent best the observed precipitation and extremes events, without losing the spatial dependency. Therefore, this probability distribution function is used to be applied with Quantile Delta Mapping (QDM) in this study (43).

In this report, QM was not applied with parametric distributions for the functions used in the mapping. This may have partly led to those results where all the climate sensitivity was lost. Additionally, the method has been criticized during recent years for several reasons (44), listed below.

- The **temporal division to perform QM**: It has been observed that relying on a calendar basis breaks some temporal distributions for rainfall, as they do not follow a monthly or a seasonal calendar. A proposition to divide BC periods based on precipitation behavior and not on calendar basis exists but is not currently applied in a method (42).
- The **stationarity assumption**: QM relies on the stationarity assumption, stating that climate characteristic from the past will stay valid in the future (44). However, this assumption is not coherent with the fact that non-stationarity is a condition for natural systems (60). Modify bias-correction methods to consider non-stationarity in biases is difficult (61). It can be noted that biases for temperature data are much more stationary than biases in precipitation data (61). However, the compliance to this stationarity assumption should be checked (44,61).
- **Corruption of values**: QM deteriorates the extremes and trends of a model by its nature and because of the stationarity assumption (44,47). In Cannon and al. (2015) (44), extremes are much higher than observed ones after BC. Therefore, by corrupting trends and extremes of the method, QM does not respect the climate sensitivity of the climate models. This can be avoided by preserving relative change signals, which is very important for precipitation climate series, or other climate variables that need to be coherent with some physical scaling relationships involving other climate variables. For example, all climate variables for atmospheric moisture need to maintain the relationship stated with Clausius-Clapeyron equation, linking water vapor and temperature (44). Detrended Quantile Mapping (DQM), Quantile Delta Mapping (QDM) or Scaled Distribution Mapping (SDM) permit to preserve relative change between past and future in trends of the climate model signals (44,47)[7].

Those three methods operate in the same way: detrend the climate series, bias correct with quantile mapping the detrended part, and reapply the climate change signal taken first on the bias corrected part (44,47). Even though DQM is based on QDM (44), DQM and QDM differ on the element detrended, and the relative changes that are preserved. DQM mapping detrend by removing the long term mean trend and permit to keep relative changes in the modelled mean, but not in the extremes. QDM detrends by quantile. Therefore, BC with QDM allow to keep

[7] QDM can be applied with the python-cmethods module and in BiasAdjustCXX command -line tool. SDM can applied with bias_correction module

relative changes in all quantiles of a distribution, but not in the mean (44). SDM is very close to QDM; it takes more in account rainfall's frequency and induvial events' frequency, and it is based on a parametric model instead of a non-parametric one in QDM (47). QDM has been recommended for BC of precipitation data, as it is not relying on stationarity assumption (43,44). Detrending before applying BC preserves the climate change signal specific to each climate model from the effects of QM (44). However, the detrended part is still corrected with QM and therefore, submitted to the stationarity condition.

All methods cited before are univariate methods. They correct climate variables independently, without taking into account the interactions between several climate variables. Moreover, they can fail to rebuild inter-variable, spatial and temporal dependencies of the observations (62). Several methods called multivariate methods exist and can be used to correctly adjust climate series while considering inter-variable corrections (62). Nevertheless, they do not reproduce well the temporal structure; the bias corrected data they are producing usually have weak temporal dependencies in comparison to observations (62). Some multivariate methods do not rely on the stationarity method, but some of them do (63).

Even knowing the QM method was not applied with a fit on parametric distribution and has defaults which are inherent to the method, even knowing that other methods could have been applied, NEX-GDDP-CMIP6 precipitation modelled data have extremes too far from reality. For example, in Figure 3-7, the maximum modelled precipitation data in Chimoio between 1985 and 2014 is around 75 mm/day, whereas for the same period and location, the maximum observed precipitation data is around 185 mm/day. It would therefore be better to take another set of data to work on precipitation indicators.

As the non-stationarity of temperature biases was not checked in this report (64), bias-corrected temperature data were not used for the temperature indicators.

3.3 Application of the methodology on Gorongosa project

3.3.1 Sensitivity

As stated in Section 2.5, sensitivity assessment of project's elements to climate variables is done with expert judgment. A workshop with the project team permitted to identify the sensitive elements of the project to climate change.

Rapid gravity sand filter, plant room, sludge holding tank and mini substation were considered sensitive to 'Incremental air temperature change'. They are all considered as assets.

Rapid gravity sand filters aim to filter water by gravity (65). Backwashing is necessary to remove solids in the filter and ensure the efficiency of the filtration (66). The actual design of backwashing is set for temperature in arrange of 15 to 30°C. Out of this range, backwashing would work less efficiently. The other elements are all sensitive to 'Incremental air temperature change' because they are composed of elements that could overheat and therefore affect their operation. The plant room and the sludge tank operate with pumps (67). Mini substation relies on transformers (element converting power to different voltage levels), that could overheat and could have a reduced carrying capacity due to higher temperature (68).

Switchgear and motors of the surface suction pumps were considered sensitive to 'Extreme temperature increase'. High air temperature can lead to an overheating of the motors, which may lead to malfunction of the pump among other effects (67,69). The switchgear is meant to protect equipment connected to a power supply from electrical overload (70). Higher temperatures can lead to switchgear failure, and then lead to power outages (71).

During the workshop, the threshold of 40°C was given as the threshold that elements subject to overheating should not exceed.

Considered as assets, sludge drying beds are sensitive to 'Incremental rainfall change'. The final drying of the sludge in this WTP relies on solar radiation. Extended periods of cumulative precipitation, with less time of solar radiation during a period could slower this process.

Nhandare river, as input of the WTP, was considered sensitive to 'Extreme rainfall change'.

Turbidity is an important aspect of WTP operation. The water turbidity of the Nhandare river, input of the WTP, could affect its operation. Turbidity is due to many different factors (e.g., discharge, presence of microorganisms). There is more turbidity during spring and summer due to algal growth, less during fall and winter because of plants' decay. A link between precipitation and turbidity was established from previous studies: periods with high turbidity are associated with the wet season, because the input of sediment and the water flow are higher, so the particles cannot settle (72). To entirely understand at which threshold of precipitation the turbidity of the Nhandare river would be affected and how, a more complete study should be done. However, it can be said that wet season and unusual events lead to more turbidity. Therefore, on-site assets and processes were considered 'Medium' sensitive to 'Extreme rainfall change' and 'incremental rainfall change'.

Floods could destroy pumps (assets). This will be assessed outside of this report.

Droughts could lead to a decrease of Nhandare river's flow (input). This was assessed in a separate hydrological study.

Strong winds could affect the mini substation, an asset of the project. The transformer of the mini substation is located outside of the building, so exposed to strong winds that could destroy it. Strong winds could also affect the power lines deserving the WTP within electricity, as it happened in March 2023 during the cyclone Freddy.

This workshop led to the establishment of the sensitivity matrix presented in the following table.

Table 3-1 - Sensitivity level for the elements of the WTP project in Gorongosa

		Sensitivity level						
Project	Sensitivity theme	Incremental air temperature change	Extreme temperature increase	Incremental rainfall change	Extreme rainfall change	Floods	Droughts	Maximum wind speed
Gorongosa	On-site assets and processes	Medium	Medium	Medium	No	Medium	No	Medium
	Inputs	No	No	Medium	Medium	No	Medium	Medium
	Output	No	No	No	No	No	No	No
	Transport links	No	No	No	No	No	No	No

3.3.2 Temperature

To better understand the exposure of the location to changes in temperature, we need to look how will evolve temperature data according to NEX-GDDP-CMIP6 in Gorongosa.

Annual mean temperature is projected to undergo a general increase between historic and future period (Table 3-2). This increase starts around 1990. Around 2050, the rate of increase between the different SSPs does not concur anymore. While ssp245, ssp370 and ssp585 projections continue to increase, ssp126's projections stay stable. Between 1990 and 2100, the annual mean temperature increases of about 1.5°C (25-23.5), and about 5.5°C (29-23.5) (Figure 3-11).

Similarly, there is an increase between past and future periods for annual maximum temperatures (Table 3-3 and Table 3-4). The trend also starts around 1990. Between 2015 and 2050, as for annual mean temperature, the SSPs have the same rate of increase. After 2050, only ssp585 and ssp370 follow the same rate of increase. The one of ssp245 decreases. The annual maximum temperature with ssp126 becomes stable after 2050 (Figure 3-12).

Number of days with a temperature exceeding 40°C is exceptional in the past; only 1 day is reported as 90th percentile. Between past and future periods, the number of day does not increase that much in the median, but it increases a lot for the highest distribution, going from 1 to 11 days in the 90th percentile (Table 3-5 and Table 3-6). After 2015, a small and similar rate of increase of the number of days is observed for every SSP. Similarly to the other indicators, around 2050, the evolution of the number of days above 40°C diverges among the SSPs. The number of days continues to increase for ssp370 and ssp585, at a higher rate for the second one. The average number of days for ssp126 and ssp245 becomes stable after 2050 (Figure 3-13).

It should be noted that for every temperature indicator, increase of temperature is between 5 and 10%, in all parts of the data distribution (Table 3-2, Table 3-3 and Table 3-4).

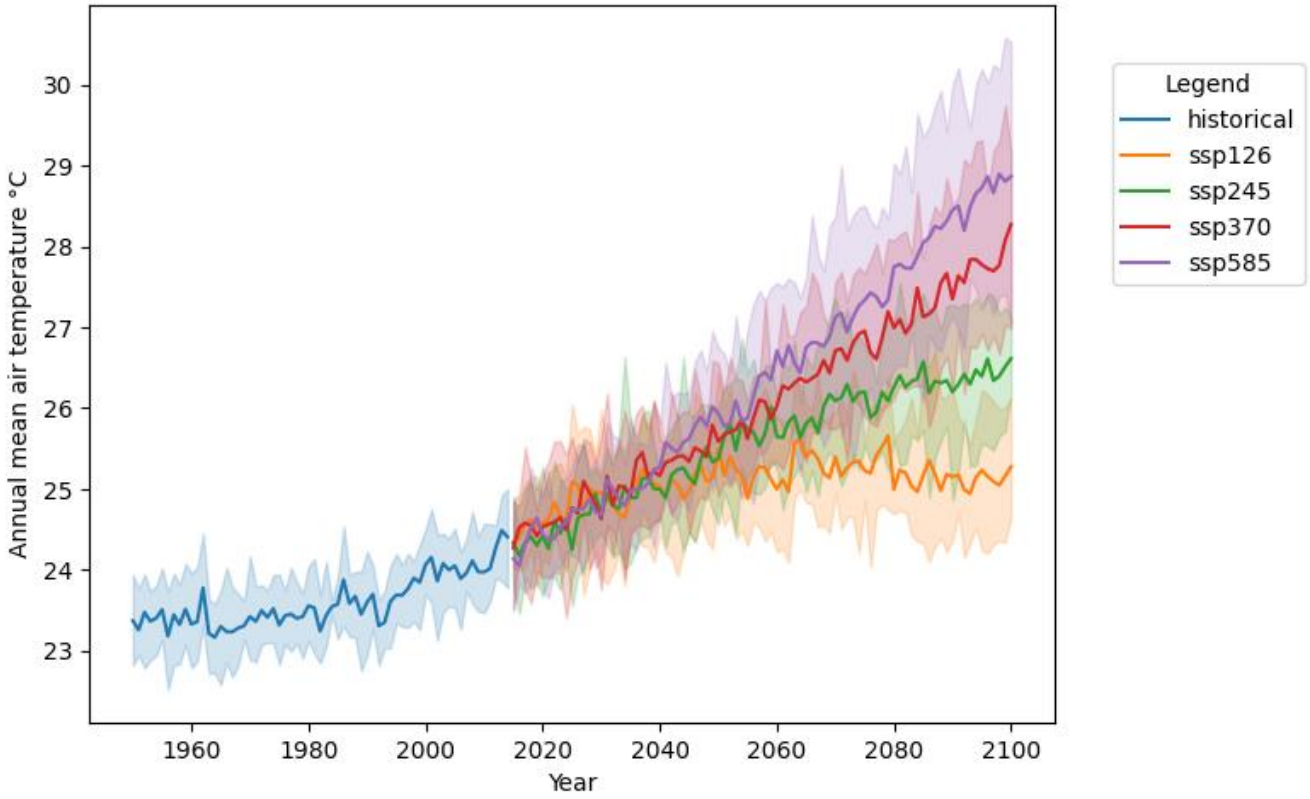

Figure 3-11 - Annual mean air temperature °C with NEX-GDDP-CMIP6 data for every scenario between 1950 and 2100 at Gorongosa. Uncertainty of each projection is due the different results from the models. The solid line is the average across the models, the shaded area represents the variation across models, between the 10th and the 90th percentile.

Table 3-2 - Statistical changes between past (1970-2014) and future (2030-2074) for mean temperature per year

Incremental air temperature change

Mean air temperature per year

	Median for the past period °C	Change in the median in %	10-th percentile for the past period °C	Change in 10-th percentile %	90-th percentile for the past period °C	Change in 90-th percentile %
Gorongosa_EIB	23.679981	7.726813	23.091981	6.188156	24.412787	9.914808

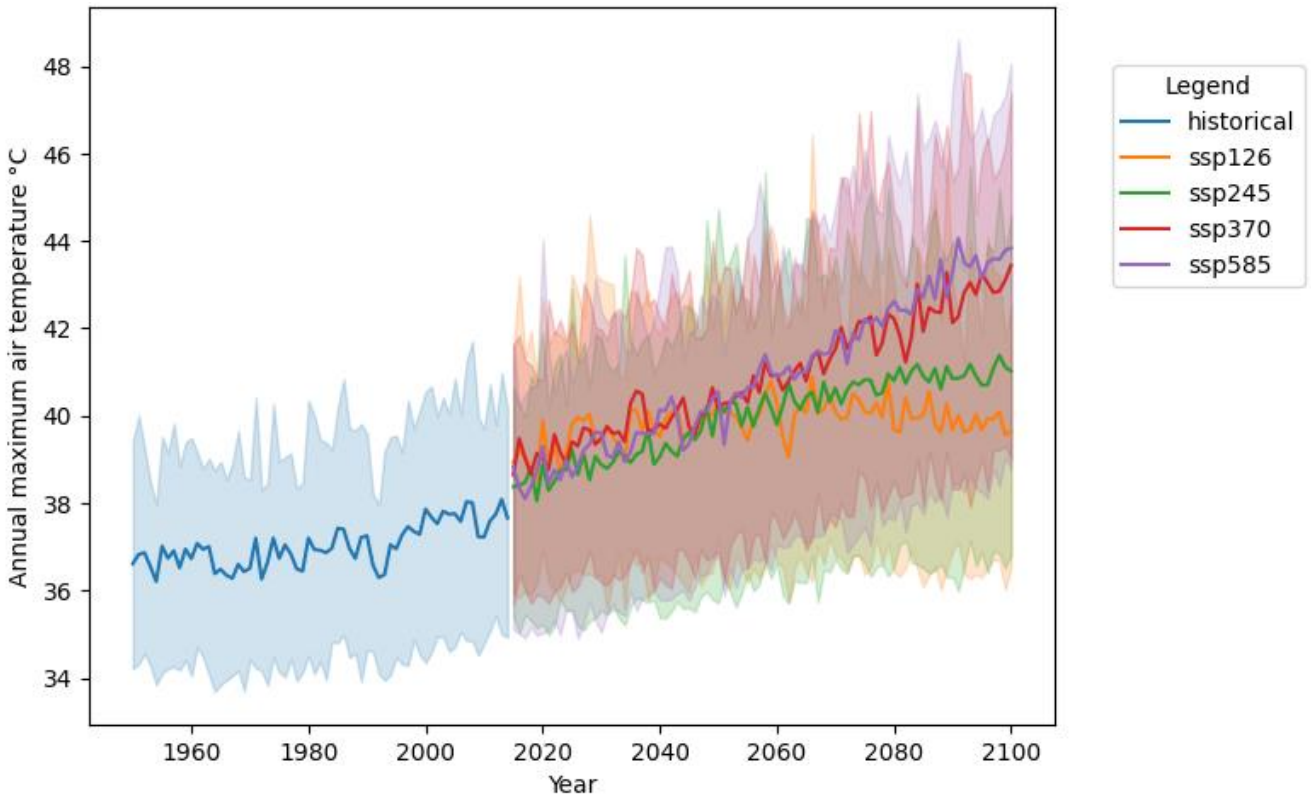

Figure 3-12 - Annual maximum of the maximum daily air temperature °C with NEX-GDDP-CMIP6 data for every scenario between 1950 and 2100 at Gorongosa. Uncertainty of each projection is due the different results from the models. The solid line is the average across the models, the shaded area represents the variation across models, between the 10th and the 90th percentile.

Table 3-3 - Statistical changes between past (1970-2014) and future (2030-2074) for Daily maximum air temperature

Extreme air temperature increase Daily maximum air temperature	Median for the past period °C	Change in the median in %	10-th percentile for the past period °C	Change in 10-th percentile %	90-th percentile for the past period °C	Change in 90-th percentile %
Gorongosa_EIB	29.008484	6.567303	24.57019	6.44491	33.540161	7.351635

Table 3-4 - Statistical changes between past (1970-2014) and future (2030-2074) for yearly maximum air temperature

Extreme air temperature increase Yearly maximum air temperature	Median for the past period °C	Change in the median in %	10-th percentile for the past period °C	Change in 10-th percentile %	90-th percentile for the past period °C	Change in 90-th percentile %
Gorongosa_EIB	38.342834	6.274504	36.475293	5.77526	40.8625	5.689313

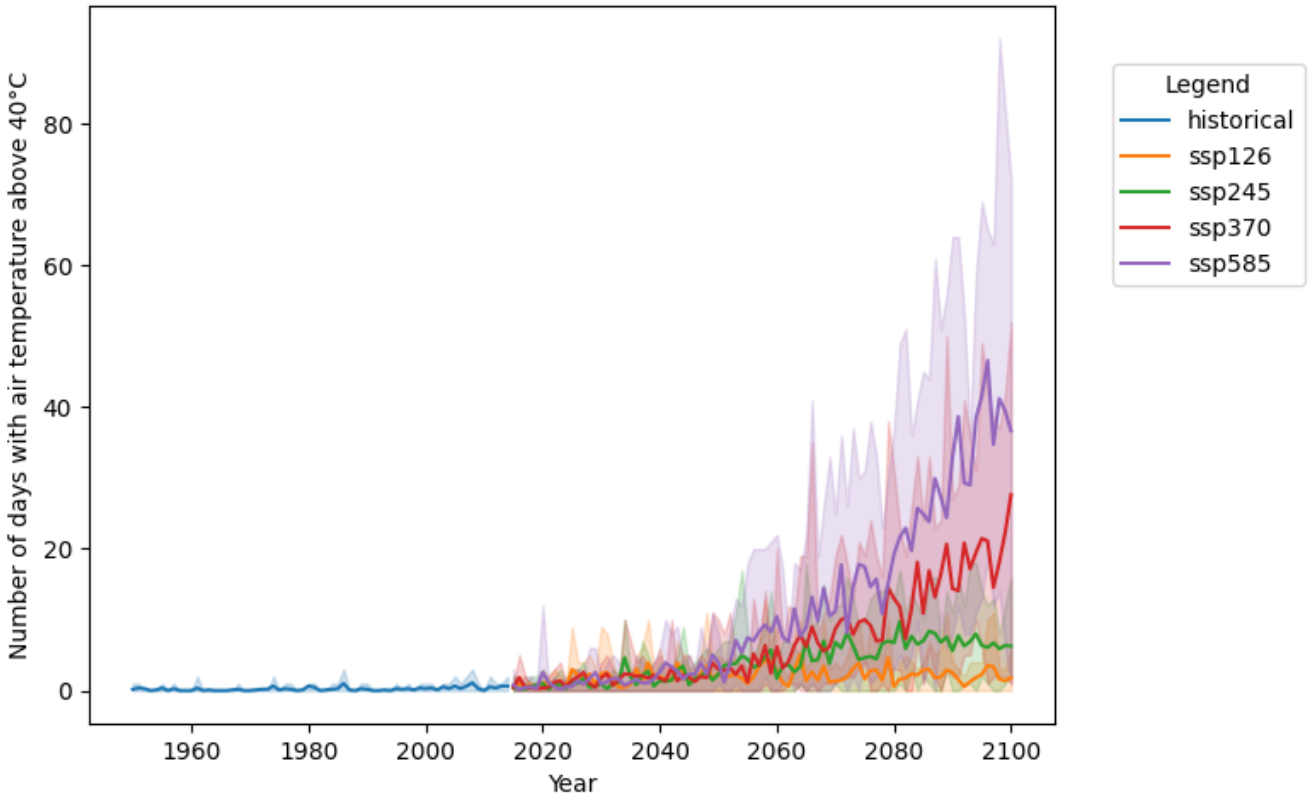

Figure 3-13 - Number of days with a maximum air temperature over 40°C with NEX-GDDP-CMIP6 data for every scenario between 1950 and 2100 at Gorongosa. Uncertainty of each projection is due the different results from the models. The solid line is the average across the models, the shaded area represents the variation across models, between the 10th and the 90th percentile.

Table 3-5 - Statistical distribution of the number of days above 40 °C for the past period (1970-2014)

	Average annual number of days with Maximum Air Temperature above 40							
	count	mean	std	min	10%	50%	90%	max
Name project								
Gorongosa_EIB	495.0	0.284848	0.695323	0.0	0.0	0.0	1.0	5.0

Table 3-6 - Statistical distribution of the number of days above 40 °C for the future period (2030-2074)

	Average annual number of days with Maximum Air Temperature above 40							
	count	mean	std	min	10%	50%	90%	max
Name project								
Gorongosa_EIB	1980.0	3.916162	6.521395	0.0	0.0	2.0	11.0	67.0

According to NEX-GDDP-CMIP6 projections, air temperature is increasing. Could this affect the sensitive elements of the WTP in Gorongosa?

As stated in section 3.3.1 - Sensitivity, some assets are sensitive to 'Incremental air temperature change' and to 'Extreme air temperature increase'. According to the methodology, some indicators must be chosen to represent those climate variable changes. To investigate evolution of 'Incremental air temperature change', the mean temperature per year was chosen as an indicator. Concerning 'Extreme air temperature increase', the 'Daily maximum air temperature' and the 'Yearly maximum air temperature' were chosen as indicators. The threshold of 40°C was given during the workshop as the critical threshold to not exceed. Therefore the 'Number of days with a maximum air temperature above 40 °C' was chosen to be part of the indicators for 'Extreme air temperature increase'.

Changes within indicators 'Daily maximum air temperature' and 'yearly maximum air temperature' were not significant (Table 3-3 and Table 3-4). Changes in 'Number of days with maximum air temperature above 40°C' could not be calculated in the same way and were therefore estimated in non-systematic way by the user. As said before, changes of the number of days above 40°C increases a lot for extremes values (90th percentile and maximum in Table 3-5 and Table 3-6). To take this change into account, the change for the 90th percentile was estimated 'Medium'.

As there was one indicator with a significant change with high uncertainty in 'Extreme air temperature increase', the final exposure was 'Medium' for this climate variable change. The indicator under 'Incremental air temperature change' did not have a significant change (Table 3-2). Therefore, there was no exposure under that climate variable change (Table 3-7).

Table 3-7 - Results for exposure levels for temperature climate variable changes

	Exposure level	
	Extreme air temperature increase	Incremental air temperature change
Gorongosa_EIB	Medium	No

Crossing the information from the sensitivity matrix with exposure matrix, it was found that assets of the Gorongosa WTP are vulnerable to 'Extreme air temperature increase' (Table 3-8).

Table 3-8 - Vulnerability level for temperature climate variable changes

		Vulnerability level	
		Incremental air temperature change	Extreme air temperature increase
Name project	Sensitivity theme		
Gorongosa_EIB	On-site assets and processes	No	Medium
	Inputs	No	No
	Output	No	No
	Transport links	No	No

As some elements are vulnerable to climate change, a risk assessment was performed as asked by the methodology. Severity of the impacts and likelihood of the events were assessed.

For this project, severity was based on expert judgment. The severity of the event 'Air temperature above 40°C' was subjectively estimated as 'Moderated'; the operation of the WTP would be affected, but not during a time too long and it can be fixed.

Concerning the likelihood, the user needed to determine the event to be evaluated. The sensitivity of the assets to extreme temperature was that the operation could be affected when the temperature reaches 40°C. How often in the future will the daily maximum temperature be over 40°C? Over the period 2030-2074, the probability of the temperature reaching values above 40°C is 1.2%, which is rare (Table 3-9). According to matrix in Table 2-4, the risk of assets malfunctioning because of temperature exceeding 40°C is therefore rare.

Table 3-9 - Probability of temperature related events during the period 2030-2074

Climate variable specifics	Indicator	Event	Probability [%]	Likelihood term
Incremental air temperature change	Average temperature per year	Annual average temperature will be above 40 °C	$6.93*10^{-6}$	Rare
Extreme temperature increase	Annual number of days with maximum temperature above 40 °C	Annual number of days above 40 °C will be more than 30	2.86	Rare
	Maximum temperature in year	The annual maximum temperature will be above 40 °C	66.29	Likely
	Daily maximum temperature	The daily maximum temperature will go above 40 °C	1.2	Rare

However, temperature exceeding 40°C could occur; the annual maximum temperature could be above 40°C with a probability of about 66%. The number of times over the year that this could probably happen is rare: the probability of the daily maximum temperature going above 40°C is only 1.2%. The mean temperature could never reach this threshold; the average temperature per year is over 40°C for the future period with a very small probability of $6.93*10^{-6}$ (Table 3-9).

3.3.3 Precipitation

Before looking at the vulnerability of the different elements, the first step is to see how could potentially evolve the precipitation at Gorongosa according to the NEX-GDDP-CMIP6 projections.

Trends for average precipitation in Gorongosa is not straightforward according to NEX-GDDP-CMIP6 projections. The general trend for annual mean precipitation seems like a decrease but is not very pronounced. However, future predictions agree on the future direction of precipitation; there is no clear different paths between the four SSPs (Figure 3-14).

'Maximum 5 days rainfall' results do not follow a clear trend either (Table 3-10). The indicator slightly increases in median and 90th percentile (respectively 3% and 1.5%) but decreases in the 10th percentile (-1.5%). The magnitude of lower values slightly decreases, while the magnitude of higher ones increases.

According to those results, magnitude of future 100-year precipitation events will increase of about 15% (median) in comparison with historical modelled data (Table 3-11). Comparing future scenarios, the uncertainty is wider for some more than for others, but there is no scenario reaching larger value than others. Additionally, there is no clear increase of the 100-year event between the two future periods (Figure 3-15).

Between the past and future period, a decrease in monthly precipitation is occurring (Table 3-12). Expect for the month of January, the historical median is always above the future median (Figure 3-16 and Figure 3-17). For future scenarios, no significative difference of behavior can be noted (Figure 3-16 and Figure 3-17).

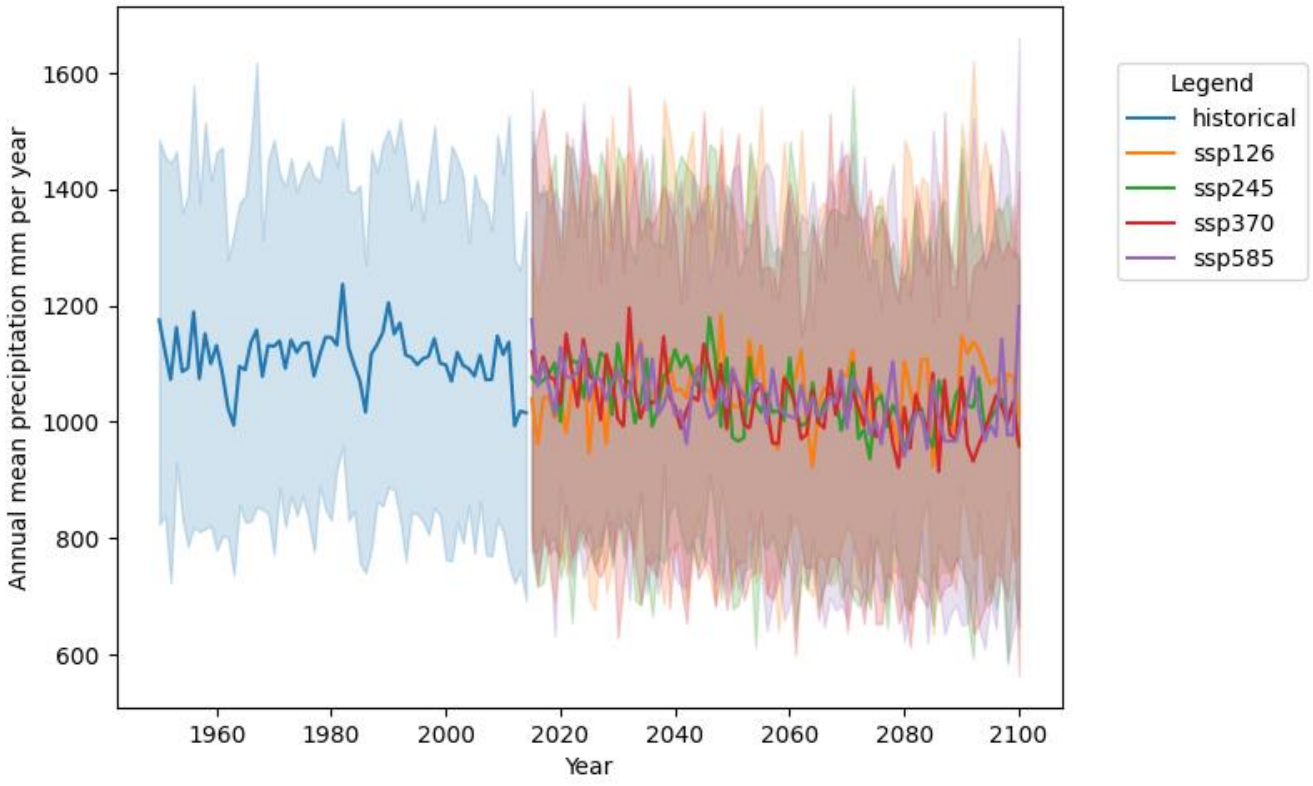

Figure 3-14 - Annual mean precipitation with NEX-GDDP-CMIP6 for every scenario between 1950 and 2100 at Gorongosa. Uncertainty of each projection is due to the different results from the models. The solid line is the average across the models, the shaded area represents the variation across models, between the 10th and the 90th percentile.

Table 3-10 - Statistical changes between past (1970-2014) and future (2030-2074) for Maximum 5 days rainfall

Extreme rainfall change Maximum five days rainfall	Median for the past period mm	Change in the median in %	10-th percentile for the past period mm	Change in 10-th percentile %	90-th percentile for the past period mm	Change in 90-th percentile %
Gorongosa_EIB	116.178371	3.078249	91.379268	-1.489684	159.246235	1.49176

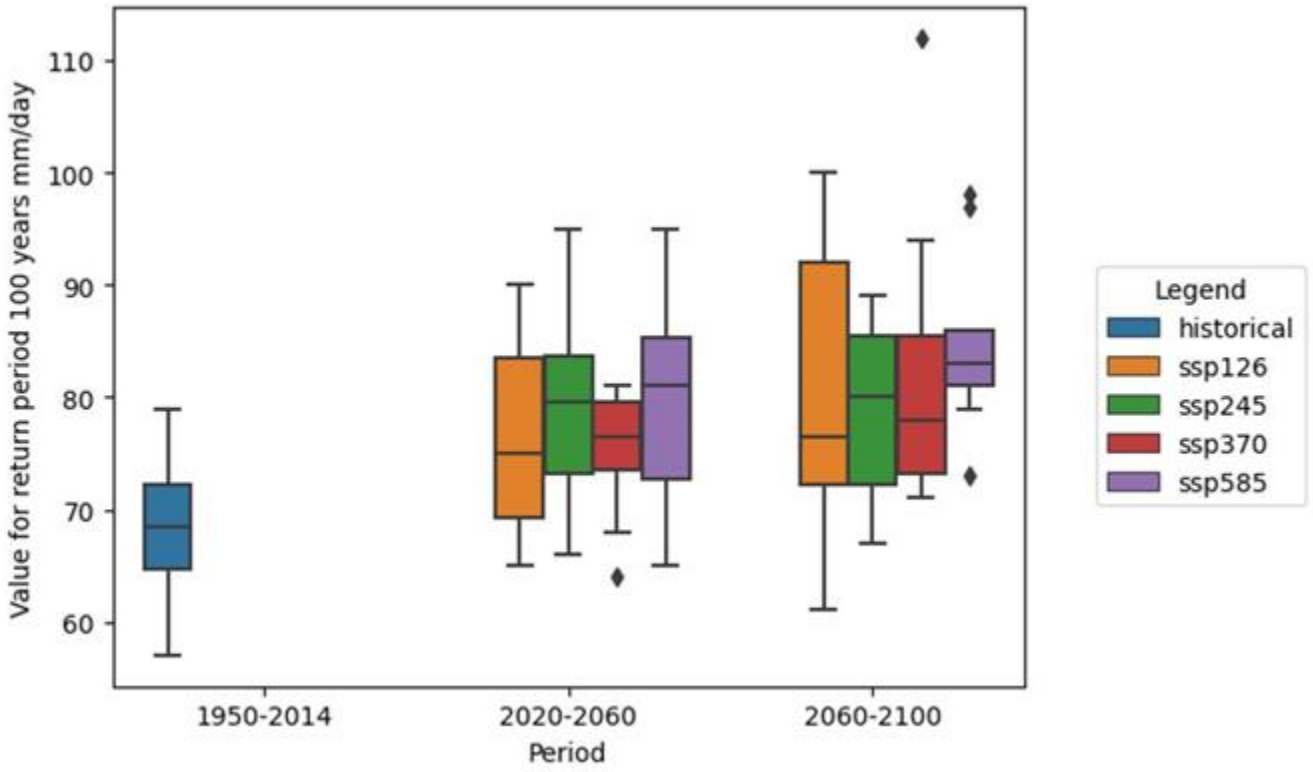

Figure 3-15 – Boxplots of 100-year precipitation event with NEX-GDDP-CMIP6 data at Gorongosa. Boxplots were categorized by experiments and periods. Historical data are from 1950 to 2014, and future projections are categorized in two periods: one from 2020 to 2060, another from 2060 to 2100. Uncertainties within each boxplot is due to the models. The boxplots are presented with the median as the central line, the 25-th/75-th percentile as first and third quartile and the 10-th percentile and the 90-th percentile as whiskers

Table 3-11 – Statistical changes between past (1970-2014) and future (2030-2074) for 100-year precipitation event

Extreme rainfall change 100 year event	Median for the past period mm/day	Change in the median in %	10-th percentile for the past period mm/day	Change in 10-th percentile %	90-th percentile for the past period mm/day	Change in 90-th percentile %
Gorongosa_EIB	68.0	15.441176	62.1	7.890499	72.9	17.969822

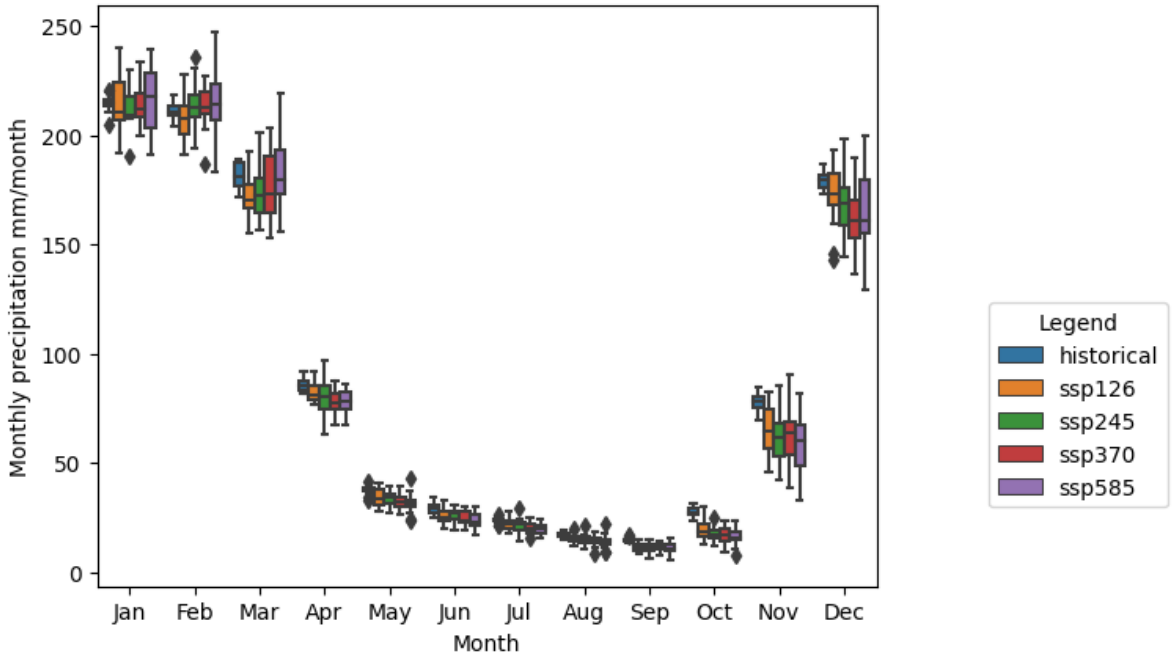

Figure 3-16- Boxplots of monthly mean precipitation with NEX-GDDP-CMIP6 data for every scenario at Gorongosa, between 1950 to 2014 for historical scenario, and between 2015 to 2100 for other scenarios. Uncertainties within each boxplot is due the different results from the models. The boxplots are presented with the median as the central line, the 25-th/75-th percentile as first and third quartile and the 10-th percentile and the 90-th percentile as whiskers

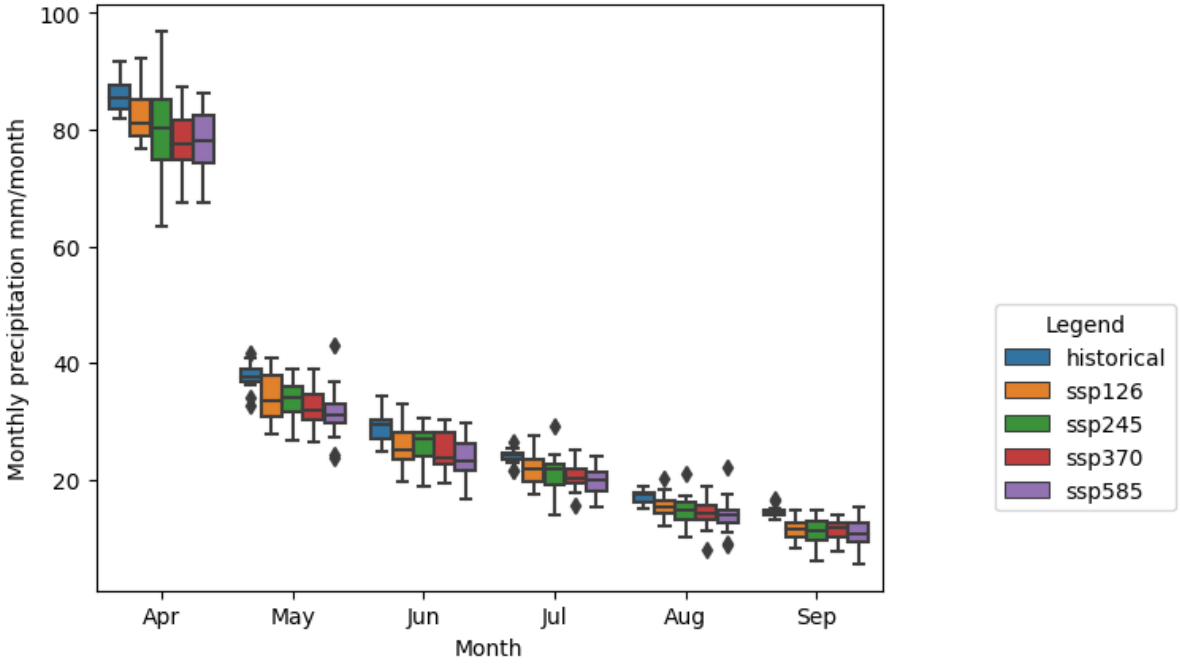

Figure 3-17 – Boxplots of monthly mean precipitation during the dry season with NEX-GDDP-CMIP6 data for every scenario at Gorongosa, between 1950 to 2014 for historical scenario, and between 2015 to 2100 for other scenarios. Uncertainties within each boxplot is due the different results from the models. The boxplots are presented with the median as the central line, the 25-th/75-th percentile as first and third quartile and the 10-th percentile and the 90-th percentile as whiskers

Table 3-12 - Statistical changes between past (1970-2014) and future (2030-2074) period for indicator 'Monthly average precipitation during wet season'

	Incremental rainfall change					
	Monthly average precipitation during wet season					
	Median for the past period mm per month	Change in the median in %	10-th percentile for the past period mm per month	Change in 10-th percentile %	90-th percentile for the past period mm per month	Change in 90-th percentile %
Gorongosa_EIB	187.802709	-10.522379	30.367685	-39.20263	234.631011	-0.589669

To determine the vulnerability of the project's elements, three indicators were analyzed for the exposure of the project's location; wet season monthly average, to represent the wet season events, and maximum five days rainfall and 100-year event, to represent the unusual events.

The two last indicators did not significantly change according to the threshold chosen (Table 3-10 and Table 3-11).

The third indicator 'wet season monthly average' was projected to significantly change between past and future with high uncertainty: there was a diminution of 39% within the 10th percentile (Table 3-12, see detailed value for past and future in Appendix C – Results). However, the change in 'wet season monthly average' could only affect the turbidity of the Nhandare river if it was increasing. This change did not lead the location to be exposed to conditions for higher turbidity. There is no exposure regarding that indicator.

There is no meaningful change for the location of the project. There is therefore no exposure for every precipitation indicator (Table 0-3). According to Table 2-3 in 2.5, when there is no exposure, even if there is a sensitivity, the elements of the project are not considered vulnerable to the evaluated climate variable changes.

Table 3-13 - Vulnerability level of elements project to precipitation climate variable changes

		Vulnerability level	
		Incremental rainfall change	Extreme rainfall change
Name project	Sensitivity theme		
Gorongosa_EIB	On-site assets and processes	No	No
	Inputs	No	No
	Output	No	No
	Transport links	No	No

3.4 Discussion of study case on Gorongosa project

3.4.1 NEX-GDDP-CMIP6 temperature projections at Gorongosa

According to results, average and maximum temperature are increasing since 1950, with an accelerated rate since 1990. Between 1960 and 2006, Mozambique has observed an increase in temperature of approximately 0.6 °C per year (73). A higher rate of increase in temperature has been observed since 1990 (22). Heat waves do not correspond exactly to the number of days above 40°C, as they correspond to three consecutive days with a daily mean temperature above the 95-th percentile of the temperature's distribution above the entire season (74). However, it should be noted that the number and intensity of heat waves has been increasing between 1983 and 2016 in Mozambique according to analysis of CHIRTS data, reanalyzing data based on in-situ and satellite observations (75). In the end, historical observations at the scale of the country agree with historical modelled data at Gorongosa.

Looking at NEX-GDDP-CMIP6 projections, temperatures will continue to increase, which is coherent with CORDEX projections (76). Those state that the future average maximum and mean temperature will be above the average of the period 1961-1990. NEX-GDDPCMIP6 and CORDEX use different notions for the scenarios: the first one use SSPs and the second RCPs. Notions are close but should be compared carefully. Temperature change with CORDEX projections is comparable with temperature change with NEX-GDDP-CMIP6 around Gorongosa. With CORDEX projections, annual mean temperature is going from 1 to 4°C increase between period 1961-1990 and 2100s periods. With NEX-GDDP-CMIP6, annual mean temperature around Gorongosa increases go from 1.5°C to 5.5°C between reference period and 2100. Regarding annual maximum temperatures around Gorongosa, CORDEX projections indicate an increase of 1 to 4°C between the reference period and the 2100s. Between the same period with NEX-GDDP-CMIP6, annual maximum temperatures increase about 2 to 8°C. Magnitudes of temperature change with NEX-GDDP-CMIP6 are larger, but in a similar order of magnitude. Looking into extreme temperature events, with high-resolution Community Earth System Model (CESM) under RCP8.5, heat waves in Mozambique are projected to go from 5 days per month to 15 days per month in average during the month of January, February, and March, which corresponds to the end of the rainy season (77). As said before, heat waves and number of days above 40°C are not the same indicator. However, the projections of increasing numbers and intensity of heat waves in Mozambique comply with the increasing number of days above 40°C (corresponding with 90th percentile of the past period in Table 3-4). Therefore, temperature projections with NEX-GDDP-CMIP6 correspond to CORDEX temperature projections and with historical observation at the scale of the country.

Divergence of NEX-GDDP-CMIP6 temperature data between SSPs corresponds to the assumptions linked to each SSP (Table 2-1).

CO_2 emissions increase effective radiative forcing, leading to an increase in temperature globally (5). Therefore, if a scenario emission assumes a certain amount of CO_2 emissions, this will impact the magnitude of temperature increase in its outputs. For example, ssp126 assumes a world reaching net-zero CO_2 emissions in 2050. Within this emission scenario, temperature becomes stable around 2050. On the contrary, ssp585 assumes a double of CO_2 emissions by 2050. Consequently, the projected temperature within this emission scenario increases a lot. As CO_2 emission assumptions between scenarios diverge, results on projected temperature also diverge.

Temperature projections in Gorongosa correspond to historical observation and CORDEX projections with a general increase of the temperature. The intensity of the warming depends on the assumption of the SSP.

3.4.2 NEX-GDDP-CMIP6 precipitation projections at Gorongosa

Precipitation projections in Gorongosa are less straightforward than temperature projections.

The historical trend from the precipitation results is hard to catch; the annual mean precipitation looks to be slightly decreasing. According to precipitation records in Mozambique, the mean annual rainfall over Mozambique decreased of 3.1% per decade between 1960 and 2006. This is mainly due to a reduction of 3.4% of rainfall per decade during the wet season (78).

Trend of future precipitation variations from results is less straightforward to describe than the result for future temperatures. The results indicate a decrease of common precipitation values and an increase of higher magnitude events at Gorongosa. Results for rainfall during wet season also project a decrease. This trend of common events having a lower magnitude and unusual events having higher magnitudes comply with the CORDEX projections. For every RCPs in (76), around Gorongosa, the annual precipitation decreases of about 20%. In another study, CORDEX confirms the trend of fewer wet days, but higher rainfall events (79).

According to CORDEX projections, for every RCPs and every period, the precipitation will decrease between 10 to 20% at Gorongosa during wet seasons. This is comparable to the 10% decrease in the median of monthly precipitation between past and future periods with NEX-GDDP-CMIP6 information.

On the contrary of general trend and monthly trend, extreme precipitation values with NEX-GDDP-CMIP6 data do not concur with observed values. In section 2.3.4 Validation of data, it was already stated that NEX-GDDP-CMIP6 precipitation data are far from reality. The 100 year-event indicator is therefore biased. Indeed, the 100-year precipitation event was calculated at Chimoio with precipitation data from the NOAA station and from the meteorological station in Gorongosa, using a Gumbel right skewed distribution as probability distribution (Result in Table 3-14). Between 1974 and 2014, the 100-year event for station Chimoio is 220 mm/day. Between 1980 and 2014, the 100-year event with Gorongosa precipitation data is 250 mm/day. According to Table 3-11, with modelled data between 1970 and 2014, the median 100-year event across climate models is 68 mm/day, varying between 62.1 (10th percentile) and 72.9 (90th percentile). Difference between past observation for this indicator as well as past modelled result are huge: 172 mm/day difference between the value in Chimoio and the result in Gorongosa with modelled data. The magnitudes of precipitation are not representative of reality.

Table 3-14 - Observed and modelled precipitation 100-year event mm/day

Observation data		**Modelled data**
At Chimoio, period 1974-2014	Gorongosa, period 1980-2014	Gorongosa, period 1970-2014
220 mm/day	250 mm/day	68 mm/day [62.1 – 72.9]

Therefore, NEX-GDDP-CMIP6 modelled precipitation data correspond to historical observation and with CORDEX projections for the general past and future trends. However, the magnitude of past extreme events with modelled data do not correspond to extreme events that were observed at Gorongosa.

3.4.3 Vulnerability, risk and climate mitigation for WTP in Gorongosa

The tool permitted to identify the sensitive elements of the project (switchgear and pumps), and to which climate variable changes those elements are vulnerable (Extreme temperature increase) as well as potential risks. Likelihood of the events indicated that temperatures will probably reach 40°C sometimes, but not very often. According to the methodology, the assets are not at risk of the temperature reaching over 40°C. However, knowing that some assets could malfunction if temperatures would go over 40°C, looking into mitigation measures is relevant. The Table 3-15 summarizes sensitivities of the project and the climate mitigation solutions that could be implemented.

Table 3-15 - Climate sensitivities of the WTP in Gorongosa and climate mitigation measures to reduce them

Climate variable changes making the assets sensitive	**Sensitive assets of the WTP**	**Climate mitigation solution**
Extreme temperature increase	Switchgear	Calibration for a higher temperature Use of a temperature-load curve
	Motors of the pumps	Reduction of power rating
Incremental temperature change	Pumps of plant room and sludge holding tank	Reduction of power rating
	Transformers of mini substation	Implementation of cooling Have transformers with more heat resistant materials
	Rapid sand filters	Adaptation of their design
Wind	Transformers of mini substation	Move them in a building

Assets vulnerable to 'Extreme temperature increase' are the switchgear and the motors of the pumps. The first one can be calibrated for a higher temperature. A temperature-load curve could also be used, which will predict

the load flow and temperature change of the switchgear according to actual conditions (71). To avoid overheating of the pump motors, their power rating should be reduced to be adapted to higher air temperature.

The pumps of the plant room and of the sludge holding tank were sensitive to 'Incremental temperature change, but not vulnerable. As said before, temperatures are going to increase. Therefore, those pumps should also be derated. Another asset sensitive but not vulnerable to 'Incremental air temperature increase' and prone to overheating because of the temperature increase are the transformers of the mini substation. To avoid overheating and reduced capacity, some cooling could be implemented. Moreover, if the actual transformers are replaced, the new ones could include more heat resistant materials (68).

Rapid gravity sand filters were not considered vulnerable to 'Incremental air temperature change' with the tool. It can be noted that their design could be changed, to have a backwashing process adapted to the new temperature range expected in the future.

Even though wind is a climate variable to which transformers of the mini substation are sensitive, the exposure and vulnerability of those assets to this climate variable was not evaluated. To reduce exposure of those elements, the transformers could be moved inside a building. Wind could also affect power lines, but this is beyond the hands of the project managers.

A cost benefit analysis could be done to determine if those changes are relevant to be implemented, regarding costs and their impacts.

The method permitted to highlight the vulnerability of the project to some climate variables, and to find mitigation solutions to improve climate-proofing of the project. The design of the method implies advantages and drawbacks, that could influence the results.

3.4.4 Advantage and drawbacks of the method

The tool is used to assess levels of vulnerability and risk for project. But it can also be used as a mean to identify elements sensitive to climate change and initiate processes of climate mitigation identification. Depending on the cost and benefits of those mitigation measures, they could be implemented and make the infrastructure less sensitive to climate change.

One other advantage is that exposure step is based on the relative change. Even if the magnitude of data is not representative of reality, if the trend of the studied data is correct, the relative change can be used and will be representative of the reality. But the risk assessment step is based on the magnitude of the value. A risk assessment with unrealistic data is therefore useless.

The method presents some drawbacks.

One of them concerns the categorization of the relative change and of the likelihood. Methodology proposed by European commission is alike methods of complete aggregation, used in Multi Criteria Decision. One of the strengths of those type of methods is the ability to make the different indicators comparable between them, by associating qualitative values to all of them (80). Moreover, the methodology permits to compare indicators without excluding one (80,81). However, aggregating elements into qualitative indicators leads to a loss of information (81). Indeed, categorizing numbers into qualitative values as done in Vulnerability and likelihood steps ended to assign two different numbers into one categorization. In the exposure step, part of vulnerability, a change of 21% between past and future in the 10th and the 90th percentile led to a categorization as 'medium'; a change of 49% between past and future in the 10th and 90th percentile led to the same categorization. In the likelihood step, probability of 0.52 and of 0.79 were both categorized as 'Likely'.

Additionally, because of the small numbers of categories, there was a strong threshold effect; a threshold effect occurs when the tipping point that leads to a sudden change is reached (82). For example, in the exposure step

(vulnerability), a change of 49% between past and future led to a medium exposure; a change of 51% between past and future led to a high exposure. Looking at the likelihood, a probability of 0.49 was labelled as 'Moderate', a probability of 0.51 was labelled as 'Likely'. To have a more precise analysis, maybe the categorization in vulnerability and likelihood should be wider but will then loose its simplicity and its straightforwardness. It should be noted that likelihood already has 5 different categories, for severity and likelihood. Even if more categories could be more precise, at same point, a trade-off should be done between precision and straightforwardness.

Some other points of the methodology could also be discussed. The threshold arbitrary chosen in the vulnerability step are sometimes too high to capture the exposition of some elements to some climate variable changes. For example, an increase of 18% of the sea level temperature during several days will lead to death of the corals (3). But this sea level temperature change will not be considered as significant according to the actual threshold settled. Moreover, the methodology does not take in account the trend of climate change to which an element can be sensitive. This is not a problem but if the analysis of the results is not done systematically, but it could be implemented in a more automatized way. Another point to improve concerns the indicator based on the number of thresholds that were overcome. In this methodology, those type if indicator does not bring so much additional information in comparison to indicators based on the value of climate variables.

4 Conclusion

As climate change impacts infrastructures, leading to direct and indirect cost damages, there is a need to identify elements of infrastructures that could be affected and increase their resilience to climate change and its negative consequences. This work presents the application of a climate vulnerability and risk assessment tool based on 'Non-paper Guidelines for Project Managers: Making vulnerable investments climate resilient' proposed by the European Commission. The method is based on the notions of sensitivity, vulnerability, hazard, and risk. The tool was applied in Mozambique, a country considered as one of the most vulnerable locations to climate change, because of its exposure to extreme climatic events and its lack of financial resources and adapted infrastructures.

This tool required the use of modelled climate projection. Produced by NASA from CMIP6 dataset, NEX-GDDP-CMIP6 dataset was chosen because it has already been bias-corrected with quantile mapping and downscaled. However, modelled maximum air temperature and precipitation revealed biases in comparison to observed data. To reduce those, quantile mapping was applied a second time using local weather data, with convincing results for maximum temperatures but not for precipitation. In this study, bias correction was performed with non-parametric distributions for its mapping, the result could be improved by performing bias correction with parametric distributions. Additionally, the method quantile delta mapping preserves better the relative changes between past and future in the quantiles of the raw climate model signal. It is therefore more adapted to use quantile delta mapping to correct precipitation data, where preserving relative changes is very important to preserve relationships with other climate variables. Moreover, stationarity being one of the main assumptions of quantile mapping, the stationarity of the biases should have been tested.

As bias correction did not perform well, NEX-GDDP-CMIP6 were used raw to evaluate how the water treatment plant project in Gorongosa could be affected by climate change.

Looking into evolution of climate projections and changes between past and future, the tool permitted to evaluate the potential evolution of climate at the project's location. According to NEX-GDDP-CMIP6 data, observations, and other projections, temperatures have been undergoing and will undergo a global increase. Average and wet season precipitation has decreased and will continue to decrease at Gorongosa. According to CORDEX precipitation projections, extreme events will have a higher intensity. Extreme precipitation data of the NEX-GDDP-CMIP6 dataset are very far from observed ones. Based on observed data and CORDEX

projections, it can be strongly assumed that the location of the water treatment plant in Gorongosa is exposed to increasing temperatures and to decreasing average precipitation, while the extreme precipitation events are increasing.

The method allows to put forward elements who are vulnerable to climate change. The tool permits to highlight the vulnerability of the pumps' motors, transformers, and switchgear to increasing temperatures. Some technical solutions could be implemented for all of them to avoid malfunctioning of the water treatment plant and improve resilience of it to climate change.

The design of the method induces some loss of information and threshold effects. Threshold value in exposure could be adapted to every climate variable. However, the method allows to identify which element of a project could be affected and how by climate change. It allows to select which climate adaptation could be implemented to increase infrastructure climate resilience. This is the final purpose of this tool.

Vulnerability and risk assessment of this CRVA method allow to assess the vulnerabilities and the risks due to climate for a project. The tool is a way to visualize vulnerability and risk, to highlight them. It could help for communication of those topics. Indeed, climate projections and risk assessments are complex to analyze and understand. But they play a crucial role in improving our understanding of future risks and enhancing climate resilience. Effective communication of these risks is essential to enable decision makers to make informed choices. This tool serves as an initial step towards facilitating this communication, by giving an overview of the future evolution of climate at the location of interest, and by highlighting the project's elements vulnerable to climate change.

5 Future research

Only temperature and precipitation were analyzed in this report. Many other climate variables could be studied. In the context of Mozambique, looking into wind and sea level rise is relevant. The country is often hit by cyclones. The sea level is increasing globally. Mozambique could be more affected than other countries by it, because more than 60% of its population live in coastal areas (23). Net precipitation could also be an interesting climate variable to investigate for WTP projects. Drying beds are sensitive to the capacity of evaporation of the air, and this could be assessed with net precipitation.

Other dataset of climate variable projections could be used. For example, the CMIP6 gathers the outputs of several GCMs under several SSPs and has more climate variables than NEX-GDDP-CMIP6[8]. Similarly, CORDEX has more climate variables in its catalogue than NEX-GDDP-CMIP6, modelled with RCMs under RCPs[9]. By using RCMs, the resolution is lower. CMIP5, former version of CMIP6, also has an extended catalogue of climate variables, outputs of GCMs under SSPs[10].

Validation of data was only based on the data from the meteorological station gathered by NOAA. Those meteorological stations are missing data for many periods. Therefore, the data used for the tool could also be compared with ERA5 dataset[11], which are reanalysis data. Reanalysis is a process combining observation and model data to propose a dataset covering the surface of the Earth and consistent with law of physics. For

[8] CMIP6 climate projections (copernicus.eu)
[9] CORDEX regional climate model data on single levels (copernicus.eu)
[10] CMIP5 daily data on single levels (copernicus.eu)
[11] ERA5 hourly data on single levels from 1940 to present (copernicus.eu)

temperature, temperature anomalies and precipitation, other datasets can be used; they were produced with algorithms like CRU or CHIRPS, using in situ and satellite data[12].

In this report, all the outputs of the NEX-GDDP-CMIP6 visually close to the distribution of observed data were selected for the analysis. The process of selection could also be done with the advanced envelope-based selection approach, a more systematic approach. This method checks if the selected GCMs perform well average and extreme climatic conditions, and if their outputs are coherent with past climate (83).

BC was not successfully applied in this report. QM could be reapplied but with a check of the stationarity of the biases and with parametric distribution for the mapping. Other methods could be applied and compared, such as QDM or SDM. According to literature, those two methods are more adapted to apply for precipitation data, because they conserve relative changes, which permits to respect the relationship with other climate variables (see section 3.2 Discussion of bias correction results).

In this report, only a few indicators were presented. Depending on the project, many other indicators can be designed and analyzed. For some projects, it may be interesting to design indicators looking into the number of consecutive days above a given threshold. For example, a heat wave corresponds to three consecutive days with a daily mean temperature above the 95-th percentile of the temperature's distribution above the entire season (74). Those heatwaves have significant impact on agriculture (84).

Indicator for the 100-return period should be improved. In this report, the 100-year event indicator was built with a right-skewed Gumbel distribution function (58), which is often done for fitting of precipitation data. The indicator would therefore maybe not apply to other climate variables, which would potentially fit better into other distribution functions. Even for precipitation, other precipitation functions could sometimes fit better: for example, Pareto, Fréchet, lognormal, Weibull or Gamma distribution functions (59).

Concerning the exposure step of the method (in vulnerability assessment), an important next milestone would be to adapt the thresholds to determine significant changes depending on the climate variable evaluated. The vulnerability step should also take into account the trend of the climate change to which the elements of the project are sensitive (positively and/or negatively), and the occurring trend of the change between past and future (positive or negative), to better estimate vulnerability.

The likelihood step (in risk assessment) could also be improved by proposing the calculation of yearly probability events. Currently, the tool only calculates probability over the period of data given as input.

[12] Temperature and precipitation gridded data for global and regional domains derived from in-situ and satellite observations (copernicus.eu)

References

1. Intergovernmental Panel on Climate Change. Changing State of the Climate System. In: Climate Change 2021 – The Physical Science Basis. Cambridge University Press; 2023. p. 287–422.
2. Intergovernmental Panel on Climate Change. Climate Change Information for Regional Impact and for Risk Assessment. In: Climate Change 2021 – The Physical Science Basis. Cambridge University Press; 2023. p. 1767–926.
3. Shivanna KR. Climate change and its impact on biodiversity and human welfare. Vol. 88, Proceedings of the Indian National Science Academy. Springer Nature; 2022. p. 160–71.
4. Intergovernmental Panel on Climate Change. Weather and Climate Extreme Events in a Changing Climate. In: Climate Change 2021 – The Physical Science Basis. Cambridge University Press; 2023. p. 1513–766.
5. Intergovernmental Panel on Climate Change. Future Global Climate: Scenario-based Projections and Near-term Information. In: Climate Change 2021 – The Physical Science Basis. Cambridge University Press; 2023. p. 553–672.
6. Intergovernmental Panel on Climate Change (IPCC). Key Risks across Sectors and Regions. In: Climate Change 2022 – Impacts, Adaptation and Vulnerability. Cambridge University Press; 2023. p. 2411–538.
7. Palin EJ, Stipanovic Oslakovic I, Gavin K, Quinn A. Implications of climate change for railway infrastructure. Vol. 12, Wiley Interdisciplinary Reviews: Climate Change. John Wiley and Sons Inc; 2021.
8. Hjort J, Streletskiy D, Doré G, Wu Q, Bjella K, Luoto M. Impacts of permafrost degradation on infrastructure. Nat Rev Earth Environ [Internet]. 2022;3(1):24–38. Available from: https://doi.org/10.1038/s43017-021-00247-8
9. Melnikov VP, Osipov VI, Brouchkov A V., Falaleeva AA, Badina S V., Zheleznyak MN, et al. Climate warming and permafrost thaw in the Russian Arctic: potential economic impacts on public infrastructure by 2050. Natural Hazards. 2022 May 1;112(1):231–51.
10. Stewart MG, Wang X, Nguyen MN. Climate change impact and risks of concrete infrastructure deterioration. Eng Struct. 2011 Apr;33(4):1326–37.
11. Chinowsky PS, Schweikert AE, Strzepek NL, Strzepek K. Infrastructure and climate change: a study of impacts and adaptations in Malawi, Mozambique, and Zambia. Clim Change. 2015 Apr 21;130(1):49–62.
12. Uamusse MM, Aljaradin M, Nilsson E, Persson KM. Climate Change observations into Hydropower in Mozambique. In: Energy Procedia [Internet]. Elsevier Ltd; 2017 [cited 2023 Aug 22]. p. 592–7. Available from: https://www.mdpi.com/2076-3417/10/14/4842
13. Adger WN, Brown I, Surminski S. Advances in risk assessment for climate change adaptation policy. Vol. 376, Philosophical Transactions of the Royal Society A: Mathematical, Physical and Engineering Sciences. Royal Society Publishing; 2018.
14. White paper: Adapting to climate change: Towards a European framework for action [Internet]. Brussels; 2009 [cited 2023 May 23]. Available from: https://eur-lex.europa.eu/LexUriServ/LexUriServ.do?uri=COM:2009:0147:FIN:EN:PDF
15. Non-paper Guidelines for Project Managers: Making vulnerable investments climate resilient.

16. Guidelines for Project Managers: Making vulnerable investments climate resilient [Internet]. 2012 [cited 2023 May 23]. Available from: https://climate-adapt.eea.europa.eu/repository/5509052.pdf

17. UNOCHA. 2018-2019 Mozambique Humanitarian Response Plan Revised following Cyclones Idai and Kenneth. 2019 May 25 [cited 2023 Aug 3]; Available from: https://reliefweb.int/report/mozambique/2018-2019-mozambique-humanitarian-response-plan-revised-following-cyclones-idai

18. World Meteorological Organization. Mozambique cyclones are "wake-up call," says WMO [Internet]. 2019 [cited 2023 Aug 3]. Available from: https://public.wmo.int/en/media/press-release/mozambique-cyclones-are-%E2%80%9Cwake-call%E2%80%9D-says-wmo

19. COWIfonden. COWIfonden-Innovative research projects [Internet]. [cited 2023 Aug 13]. Available from: https://www.cowifonden.com/donations/application-guidelines/innovative-research-projects

20. COWIfonden. COWIfonden - Bevillinger 2023 [Internet]. [cited 2023 Aug 13]. Available from: https://www.cowifonden.dk/donationer/nyere-projekter/bevillinger-2023

21. Baez JE, Caruso G, Niu C. Tracing Back the Weather Origins of Human Welfare Evidence from Mozambique [Internet]. 2017. Available from: http://econ.worldbank.org.

22. The World Bank Group. Mozambique - Current climate > Climatology [Internet]. 2021 [cited 2023 Aug 27]. Available from: https://climateknowledgeportal.worldbank.org/country/mozambique/climate-data-historical

23. Mucova SAR, Azeiteiro UM, Filho WL, Lopes CL, Dias JM, Pereira MJ. Approaching sea-level rise (Slr) change: Strengthening local responses to sea-level rise and coping with climate change in northern mozambique. J Mar Sci Eng. 2021 Feb 1;9(2):1–17.

24. The Intergovernmental Panel on Climate Change. The Intergovernmental Panel on Climate Change [Internet]. 2023 [cited 2023 Jul 27]. Available from: https://www.ipcc.ch/

25. Intergovernmental Panel on Climate Change (IPCC). Glossary. In: Climate Change 2022 – Impacts, Adaptation and Vulnerability [Internet]. Cambridge University Press; 2023 [cited 2023 Jul 27]. p. 2897–930. Available from: https://www.ipcc.ch/report/ar6/wg2/downloads/report/IPCC_AR6_WGII_Annex-II.pdf

26. Mechoso CR, Arakawa A. Numerical Models: General Circulation Models. In: Encyclopedia of Atmospheric Sciences: Second Edition. Elsevier Inc.; 2015. p. 153–60.

27. Wu Y, Miao C, Fan X, Gou J, Zhang Q, Zheng H. Quantifying the Uncertainty Sources of Future Climate Projections and Narrowing Uncertainties With Bias Correction Techniques. Earths Future [Internet]. 2022 Nov 1 [cited 2023 Aug 22];10(11). Available from: https://agupubs.onlinelibrary.wiley.com/doi/epdf/10.1029/2022EF002963

28. Intergovernmental Panel on Climate Change. Framing, Context, and Methods. In: Climate Change 2021 – The Physical Science Basis [Internet]. Cambridge University Press; 2023 [cited 2023 Jul 27]. p. 147–286. Available from: https://www.ipcc.ch/report/ar6/wg1/downloads/report/IPCC_AR6_WGI_Chapter01.pdf

29. Intergovernmental Panel on Climate Change. Linking Global to Regional Climate Change. In: Climate Change 2021 – The Physical Science Basis. Cambridge University Press; 2023. p. 1363–512.

30. Copernicus, Programme of the European Union, ECMWF. ECMWF-CMIP6: Global climate projections [Internet]. [cited 2023 Aug 14]. Available from:

https://confluence.ecmwf.int/display/CKB/CMIP6%3A+Global+climate+projections#CMIP6:Globalclimateprojections-Models

31. O'Neill BC, Kriegler E, Ebi KL, Kemp-Benedict E, Riahi K, Rothman DS, et al. The roads ahead: Narratives for shared socioeconomic pathways describing world futures in the 21st century. Global Environmental Change. 2017 Jan 1;42:169–80.

32. ES-DOC Earth System Documentation. ES-DOC Earth System Documentation - Simulations [Internet]. [cited 2023 Aug 3]. Available from: https://es-doc.org/cmip6-ensembles-simulations/

33. Schwarzwald K, Lenssen N, by Timothy Palmer E. The importance of internal climate variability in climate impact projections. 2022; Available from: https://doi.org/10.1073/pnas.2208095119

34. Nyenzi B, Lefale PF. El NiñoNi˜Niño Southern Oscillation (ENSO) and global warming. Vol. 6, Advances in Geosciences. 2006.

35. Copernicus, ECMWF. CMIP6 Climate projections. [cited 2023 Aug 3]; Available from: https://cds.climate.copernicus.eu/cdsapp#!/dataset/projections-cmip6?tab=overview

36. NOAA. Global Historical Climatology Network daily (GHCNd). [cited 2023 Aug 3]; Available from: https://www.ncei.noaa.gov/products/land-based-station/global-historical-climatology-network-daily

37. NOAA. NOAA - About our agency. 2023 Mar 2 [cited 2023 Aug 3]; Available from: https://www.noaa.gov/about-our-agency

38. NOAA. GHCN (Global Historical Climatology Network)-Daily Documentation [Internet]. [cited 2023 Aug 3]. Available from: https://www.ncei.noaa.gov/pub/data/cdo/documentation/GHCND_documentation.pdf

39. Thrasher B, Wang W, Michaelis A, Melton F, Lee T, Nemani R. NASA Global Daily Downscaled Projections, CMIP6. Sci Data. 2022 Dec 1;9(1).

40. Loff Sarah, Dunbar Brian. https://www.nasa.gov/about/index.html. 2023. About NASA.

41. WMO - World meteorological organization. WMO is monitoring potential new temperature records [Internet]. 2022 [cited 2023 Aug 15]. Available from: https://public.wmo.int/en/media/news/wmo-monitoring-potential-new-temperature-records

42. Bum Kim K, Bray M, Han D. An improved bias correction scheme based on comparative precipitation characteristics. 2014.

43. Heo JH, Ahn H, Shin JY, Kjeldsen TR, Jeong C. Probability distributions for a quantile mapping technique for a bias correction of precipitation data: A case study to precipitation data under climate change. Water (Switzerland). 2019 Jul 1;11(7).

44. Cannon AJ, Sobie SR, Murdock TQ. Bias correction of GCM precipitation by quantile mapping: How well do methods preserve changes in quantiles and extremes? J Clim [Internet]. 2015 [cited 2023 Aug 22];28(17):6938–59. Available from: https://journals.ametsoc.org/view/journals/clim/28/17/jcli-d-14-00754.1.xml

45. Schwertfeger BT, Lohmann G, Lipskoch H. Introduction of the BiasAdjustCXX command-line tool for the application of fast and efficient bias corrections in climatic research. SoftwareX [Internet]. 2023 May 1 [cited 2023 Aug 22];22. Available from: https://www.softxjournal.com/article/S2352-7110(23)00075-4/fulltext

46. Luo M, Liu T, Meng F, Duan Y, Frankl A, Bao A, et al. Comparing bias correction methods used in downscaling precipitation and temperature from regional climate models: A case study from the Kaidu River Basin in Western China. Water (Switzerland) [Internet]. 2018 Aug 7 [cited 2023 Aug 22];10(8). Available from: https://www.mdpi.com/2073-4441/10/8/1046

47. Switanek BM, Troch AP, Castro LC, Leuprecht A, Chang HI, Mukherjee R, et al. Scaled distribution mapping: A bias correction method that preserves raw climate model projected changes. Hydrol Earth Syst Sci [Internet]. 2017 Jun 6 [cited 2023 Aug 22];21(6):2649–66. Available from: https://hess.copernicus.org/articles/21/2649/2017/

48. Jakob Themeßl M, Gobiet A, Leuprecht A. Empirical-statistical downscaling and error correction of daily precipitation from regional climate models. International Journal of Climatology. 2011 Aug;31(10):1530–44.

49. Teutschbein C, Seibert J. Bias correction of regional climate model simulations for hydrological climate-change impact studies: Review and evaluation of different methods. J Hydrol (Amst). 2012 Aug 16;456–457:12–29.

50. A LM. Exploring quantile mapping as a tool to produce user-tailored climate scenarios for Switzerland [Internet]. 2018. Available from: www.meteoschweiz.ch

51. Wood AW, Leung LR, Sridhar V, Lettenmaier DP. HYDROLOGIC IMPLICATIONS OF DYNAMICAL AND STATISTICAL APPROACHES TO DOWNSCALING CLIMATE MODEL OUTPUTS. 2004.

52. Gutiérrez JM, Maraun D, Widmann M, Huth R, Hertig E, Benestad R, et al. An intercomparison of a large ensemble of statistical downscaling methods over Europe: Results from the VALUE perfect predictor cross-validation experiment. International Journal of Climatology. 2019 Jul 1;39(9):3750–85.

53. scikit-downscale GitHub [Internet]. 2022 [cited 2023 Aug 20]. Available from: https://github.com/pangeo-data/scikit-downscale/tree/main

54. Joe Hamman. Scikit-downscale: toolkit for statistical downscaling [Internet]. 2020 [cited 2023 Aug 20]. Available from: https://scikit-downscale.readthedocs.io/en/latest/

55. scikit-learn 1.3.0 [Internet]. [cited 2023 Aug 20]. Available from: https://pypi.org/project/scikit-learn/

56. scikit-learn - Machine Learning in Python [Internet]. [cited 2023 Aug 20]. Available from: https://scikit-learn.org/stable/index.html

57. Commission notice - Technical guidance on the climate proofing of infrastructure in the period 2021-2027. Official Journal of the European Commision. 2021 Sep 16;

58. The Scipy community. scipy.stats.gumbel_r [Internet]. [cited 2023 Aug 20]. Available from: https://docs.scipy.org/doc/scipy/reference/generated/scipy.stats.gumbel_r.html

59. Moccia B, Mineo C, Ridolfi E, Russo F, Napolitano F. Probability distributions of daily rainfall extremes in Lazio and Sicily, Italy, and design rainfall inferences. J Hydrol Reg Stud [Internet]. 2021 Feb 1 [cited 2023 Aug 20];33. Available from: https://www.sciencedirect.com/science/article/pii/S2214581820302457

60. Grillakis MG, Koutroulis AG, Daliakopoulos IN, Tsanis IK. Addressing the assumption of stationarity in statistical bias 1 correction of temperature. Manuscript under review for journal Earth Syst Dynam

[Internet]. 2016 [cited 2023 Aug 22];27. Available from: https://esd.copernicus.org/preprints/esd-2016-52/esd-2016-52.pdf

61. Nahar J, Johnson F, Sharma A. Assessing the extent of non-stationary biases in GCMs. J Hydrol (Amst) [Internet]. 2017 Jun 1 [cited 2023 Aug 22];549:148–62. Available from: https://www.sciencedirect.com/science/article/pii/S0022169417301919?ref=pdf_download&fr=RR-2&rr=7facf5b1dae57373

62. François B, Vrac M, Cannon A, Robin Y, Allard D, Cannon AJ. Multivariate bias corrections of climate simulations: which benefits for which losses? Earth Syst Dynam [Internet]. 2020;11:537–62. Available from: https://doi.org/10.5194/esd-11-537-2020

63. Cannon AJ. Multivariate quantile mapping bias correction: an N-dimensional probability density function transform for climate model simulations of multiple variables. Clim Dyn [Internet]. 2018 Jan 1 [cited 2023 Aug 22];50(1–2):31–49. Available from: https://link.springer.com/article/10.1007/s00382-017-3580-6

64. Chen J, Brissette FP, Lucas-Picher P. Assessing the limits of bias-correcting climate model outputs for climate change impact studies. J Geophys Res [Internet]. 2015 Feb 16 [cited 2023 Aug 22];120(3):1123–36. Available from: https://agupubs.onlinelibrary.wiley.com/doi/epdf/10.1002/2014JD022635

65. Sarma J. Chapter 6 - Filtration and chemical treatment of waterborne pathogens. In: Vara Prasad MN, Grobelak A, editors. Waterborne Pathogens [Internet]. Butterworth-Heinemann; 2020. p. 105–22. Available from: https://www.sciencedirect.com/science/article/pii/B9780128187838000062

66. Wang D, Zhou J, Lin H, Chen J, Qi J, Bai Y, et al. Impacts of backwashing on micropollutant removal and associated microbial assembly processes in sand filters. Front Environ Sci Eng. 2023 Mar 1;17(3).

67. Jee pumps. Pump overheating - Causes, symptoms and mitigation [Internet]. 2023 [cited 2023 Aug 27]. Available from: https://www.jeepumps.com/pump-overheating-causes-symptoms-and-mitigation/

68. Burillo D. Effects of Climate Change in Electric Power Infrastructures. In: Power System Stability [Internet]. IntechOpen; 2019 [cited 2023 Aug 27]. Available from: https://www.intechopen.com/chapters/64723

69. Grundfos. What leads to overheating of motors ? [Internet]. [cited 2023 Aug 27]. Available from: https://www.grundfos.com/solutions/support/faq/what-leads-to-overheating-of-motors

70. ASCO. What is a switchgear ? [Internet]. 2023 [cited 2023 Aug 27]. Available from: https://www.ascopower.com/us/en/resources/articles/what-is-switchgear.jsp

71. Yang R, Li T, Chen J, Lin J, Mao L, Wang M. Research and Application of Temperature Load of Switchgear. In: Journal of Physics: Conference Series. Institute of Physics; 2022.

72. Göransson G, Larson M, Bendz D. Variation in turbidity with precipitation and flow in a regulated river system-river Göta Älv, SW Sweden. Hydrol Earth Syst Sci [Internet]. 2013 [cited 2023 Aug 17];17(7):2529–42. Available from: https://hess.copernicus.org/articles/17/2529/2013/hess-17-2529-2013.pdf

73. McSweeney. UNDP climate change profile for Mozambique. 2010.

74. Zacharias S, Koppe C, Mücke HG. Climate change effects on heat waves and future heat wave-associated IHD mortality in Germany. Climate. 2015 Mar 1;3(1):100–17.

75. Pereira Marghidan C, van Aalst M, Blanford J, Guigma K, Pinto I, Maure G, et al. Heatwaves in Mozambique 1983–2016: Characteristics, trends and city-level summaries using high-resolution CHIRTS-daily. Weather Clim Extrem. 2023 Jun 1;40.

76. Mavume AF, Banze BE, Macie OA, Queface AJ. Analysis of climate change projections for mozambique under the representative concentration pathways. Atmosphere (Basel). 2021;12(5).

77. Asefi-Najafabady S, Vandecar KL, Seimon A, Lawrence P, Lawrence D. Climate change, population, and poverty: vulnerability and exposure to heat stress in countries bordering the Great Lakes of Africa. Clim Change. 2018 Jun 1;148(4):561–73.

78. Uamusse MM, Tussupova K, Persson KM. Climate change effects on hydropower in Mozambique. Applied Sciences (Switzerland) [Internet]. 2020 Jul 1 [cited 2023 Aug 20];10(14). Available from: https://www.mdpi.com/2076-3417/10/14/4842

79. Abiodun BJ, Mogebisa TO, Petja B, Abatan AA, Roland TR. Potential impacts of specific global warming levels on extreme rainfall events over southern Africa in CORDEX and NEX-GDDP ensembles. International Journal of Climatology. 2020 May 1;40(6):3118–41.

80. Keeney RL, Raiffa H. Decision Making with Multiple Objectives Preferences and Value Tradeoffs. Wiley, New York. 1976.

81. Hassan Zardari Kamal Ahmed Sharif Moniruzzaman Shirazi Zulkifli Bin Yusop N. SPRINGER BRIEFS IN WATER SCIENCE AND TECHNOLOGY Weighting Methods and their Effects on Multi-Criteria Decision Making Model Outcomes in Water Resources Management [Internet]. Available from: http://www.springer.com/series/11214

82. Tang B sin, Wong KT. Threshold effects of incremental redevelopment of an industrial property on a residential neighbourhood. Landsc Urban Plan. 2021 Apr 1;208.

83. Lutz AF, ter Maat HW, Biemans H, Shrestha AB, Wester P, Immerzeel WW. Selecting representative climate models for climate change impact studies: an advanced envelope-based selection approach. International Journal of Climatology [Internet]. 2016 Oct 1 [cited 2023 Aug 23];36(12):3988–4005. Available from: https://rmets.onlinelibrary.wiley.com/doi/full/10.1002/joc.4608

84. Kumar R, Raj Gautam H. Climate Change and its Impact on Agricultural Productivity in India. Journal of Climatology & Weather Forecasting. 2014;2(1).

Appendix A – Detail procedure of downscaling to produce NEX-GDDP-CMIP6

Detailed procedure:

1. **Treatment of GMFD**: GFMD data at resolution ¼ degree are smoothed.
2. Interpolation of GMFD to have the same resolution as GCM models outputs.
3. **Obtain relative changes of BC GCMs**, by subtracting the output from step 2 to the bias corrected GCMs outputs for temperature data, and by dividing the bias corrected GCMs outputs by the output from step 2 for other variables.
4. The relative changes are then bilinearly **interpolated to the original ¼ degree resolution** of GMFD.
5. **Obtain final downscaled product**, by adding the output of step 1 to the relative changes (output step 4) for the temperature variables, by multiplying the output step 1 by the relative changes (output step 4) for other climate variables.

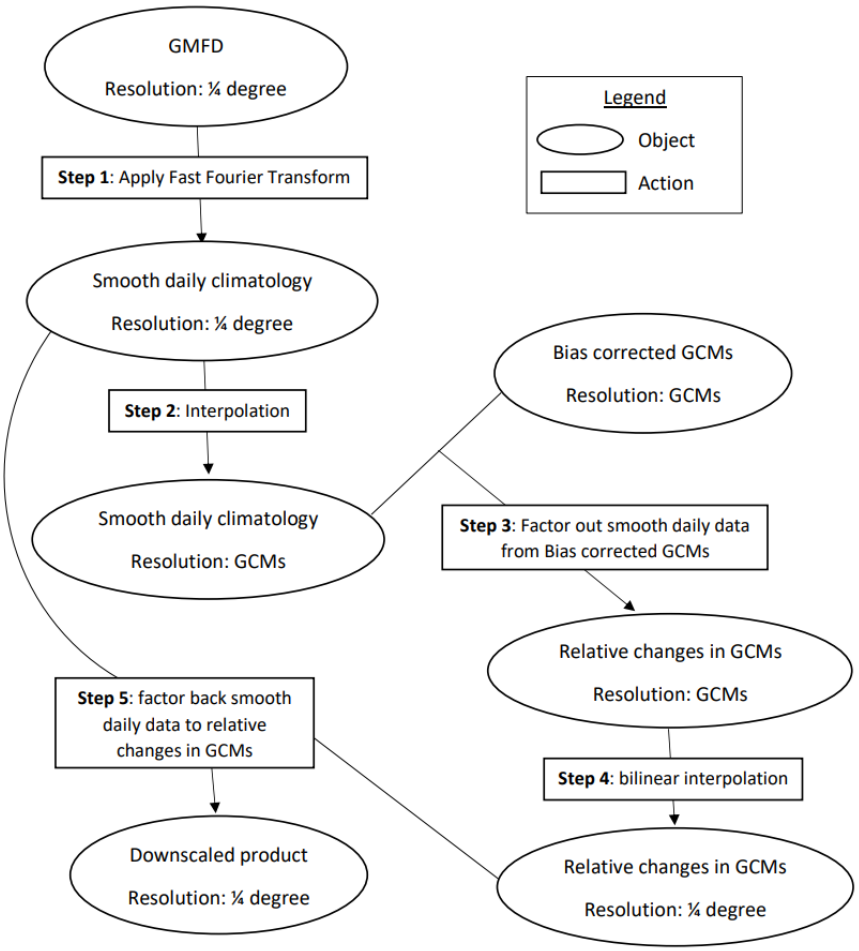

Figure 0-1 - Scheme of the spatial disaggregation used in Trasher 2022 (39)

Appendix B – Validation of NEX-GDDP-CMIP6 data

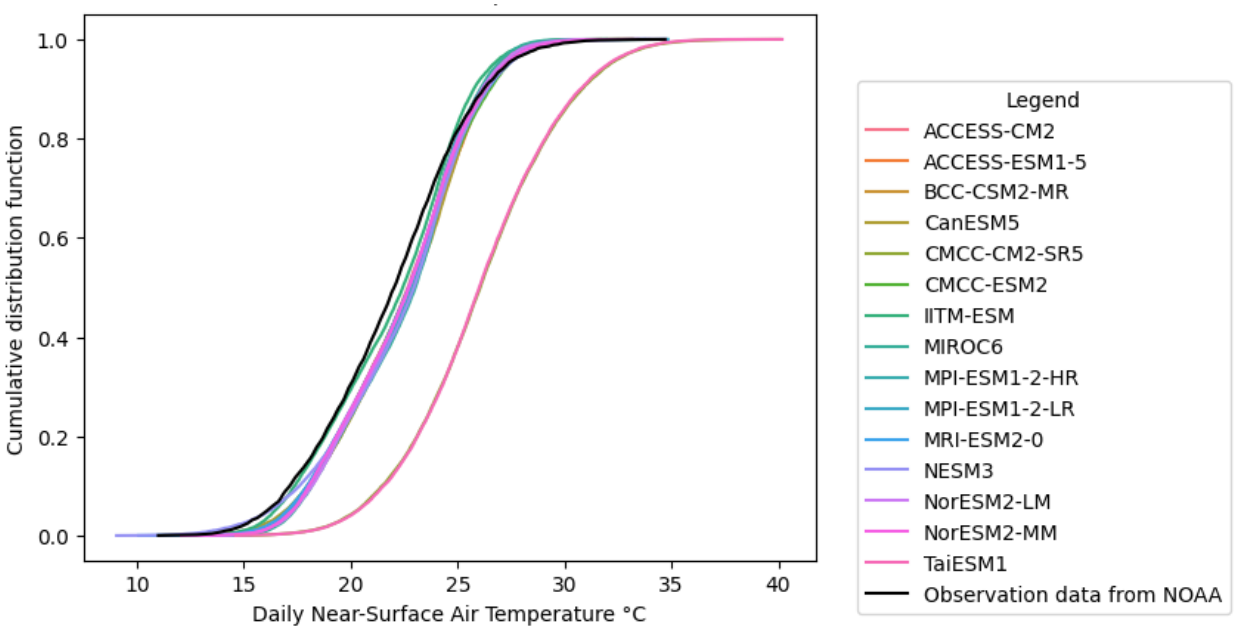

Figure 0-1 - CDFs of NEX-GDDP-CMIP6 modelled daily air temperature °C, compared to CDF of observed temperature data. All data are between 1970 and 2014 and are in Chimoio. Each colored line represents the CDF for the output data of a GCM. The black line is the CDF of the observed data at the meteorological station in Chimoio. All models are following the observed distribution, except the models TaiESM1 and CMCC-CM2-SR5.

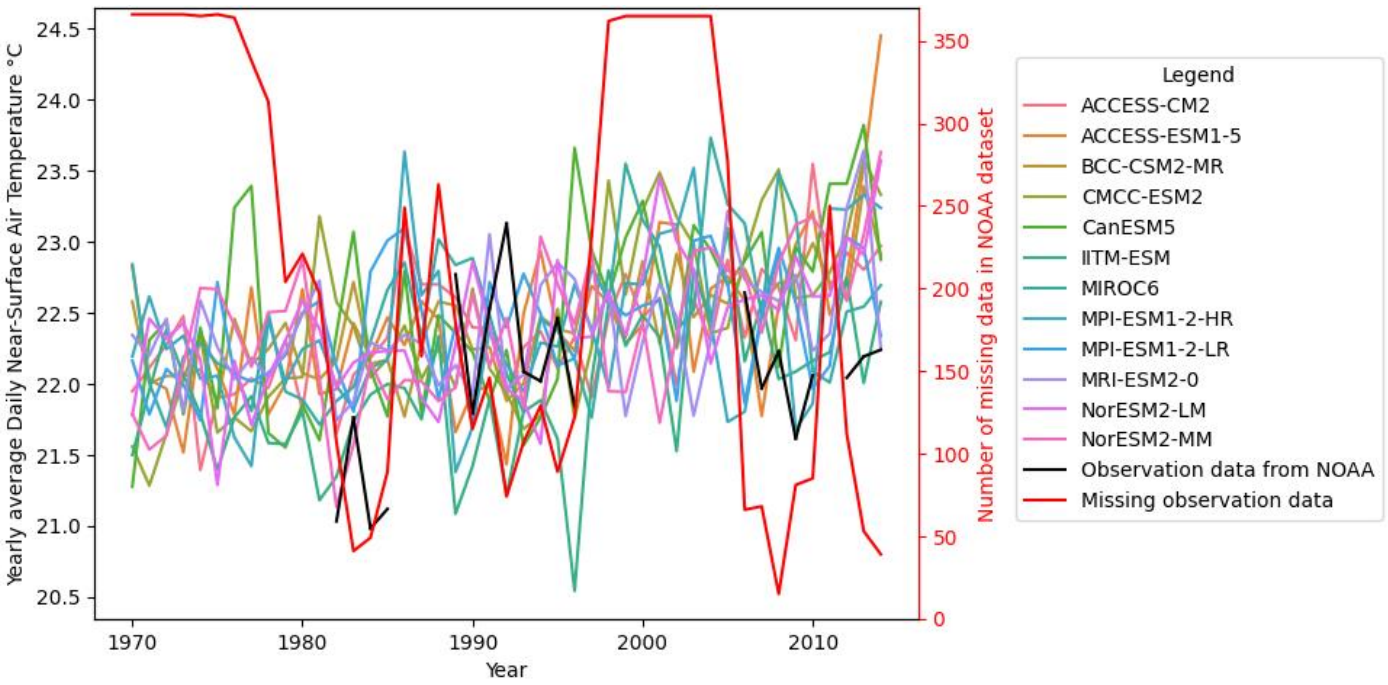

Figure 0-2 -Annual average air temperature °C between 1970 and 2014 in Chimoio. Each colored line represents the output of one model, the black line represents the observed value. Those lines should be read with the left y-axis. The red line presents the number of missing data per year. It should be read with the right y-axis If a year is missing more than half of the observed value, the value of the observed data (black line) is not displayed. Between 1970 and 2014, 60% of the observed data are missing. Observed annual average temperature concur with modelled ones.

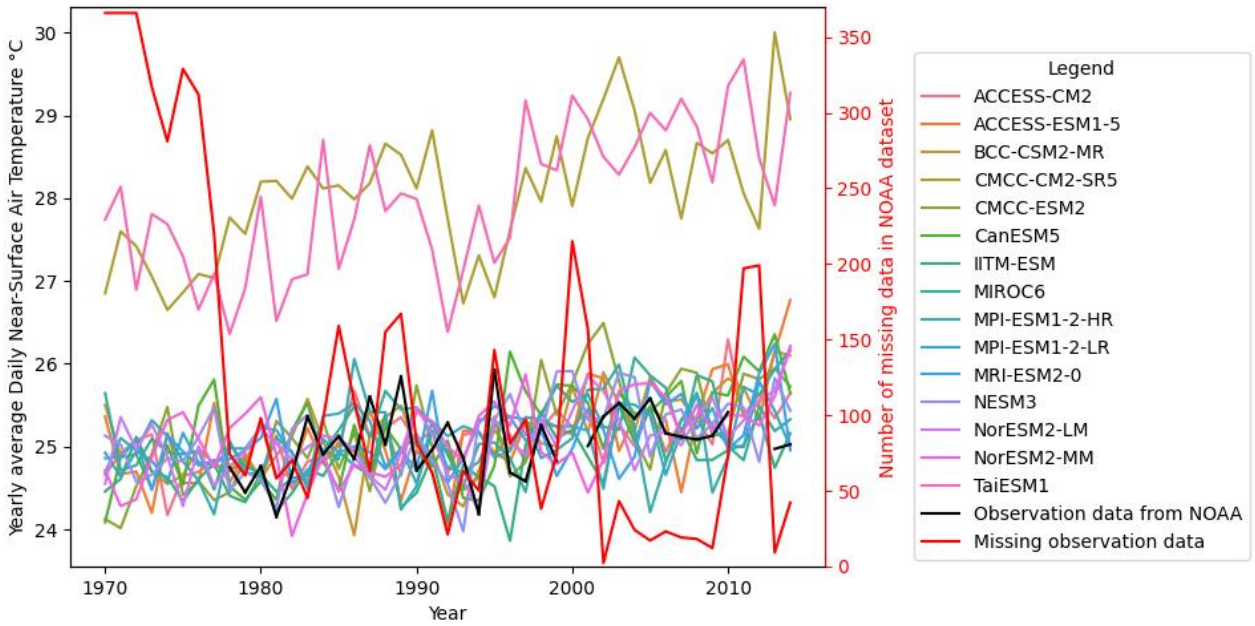

Figure 0-3 - Annual average air temperature °C between 1970 and 2014 in Beira. Each colored line represents the output of one model, the black line represents the observed value. Those lines should be read with the left y-axis. The red line presents the number of missing data per year. It should be read with the right y-axis If a year is missing more than half of the observed value, the value of the observed data (black line) is not displayed. Between 1970 and 2014, 50% of the observed data are missing. Observed annual average temperature concur with modelled ones.

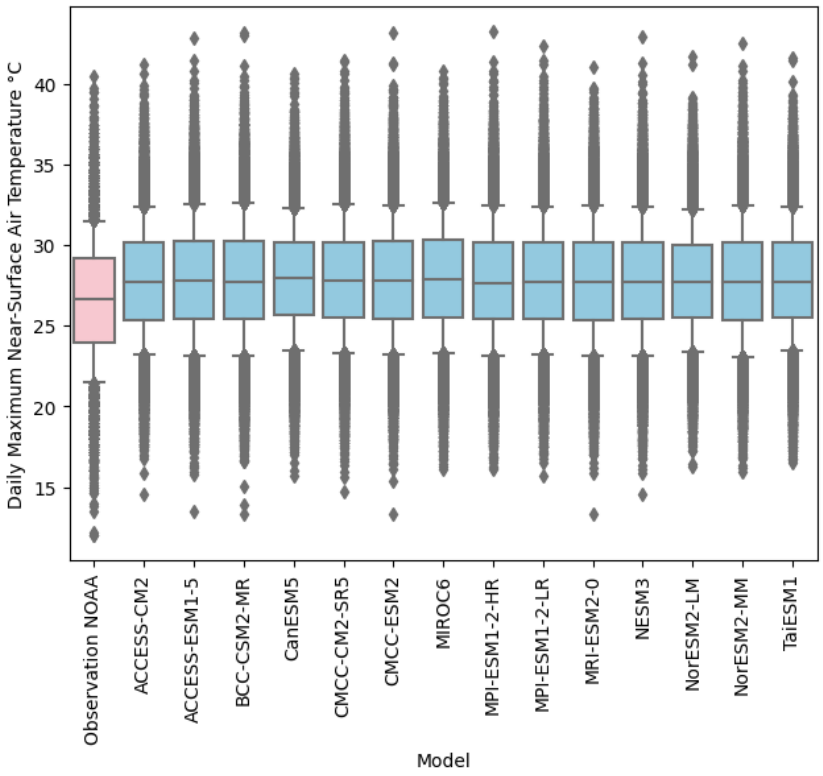

Figure 0-4 - Boxplots of the NEX-GDDP-CMIP6 modelled daily maximum temperature °C (in blue), compared to the boxplot of the daily maximum temperature °C registered by the meteorological station (in pink). Data are between 1970 and 2014 and are from Chimoio. The boxplots are presented with the median as the central line, the 25-th/75-th percentile as first and third quartile, the 10-th percentile and the 90-th percentile as whiskers and with outliers. The trends between observed and modelled data concur.

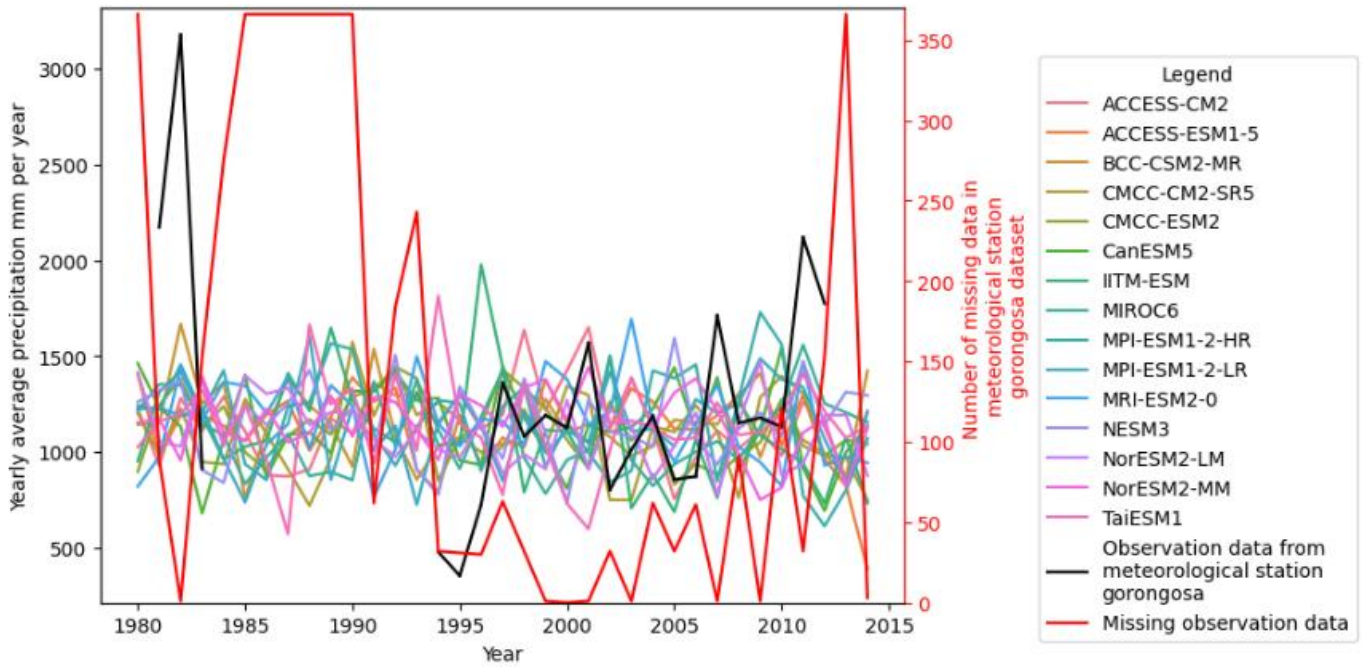

Figure 0-5 - Annual average precipitation mm/year between 1980 and 2014 in Gorongosa. Each colored line represents the output of one model, the black line represents the observed value. Those lines should be read with the left y-axis. The red line presents the number of missing data per year. It should be read with the right y-axis. If a year is missing more than half of the observed value, the value of the observed data (black line) is not displayed. Between 1980 and 2014, 35% of the observed data are missing. Observed annual average temperature concur with modelled ones for the period 1995-2014.

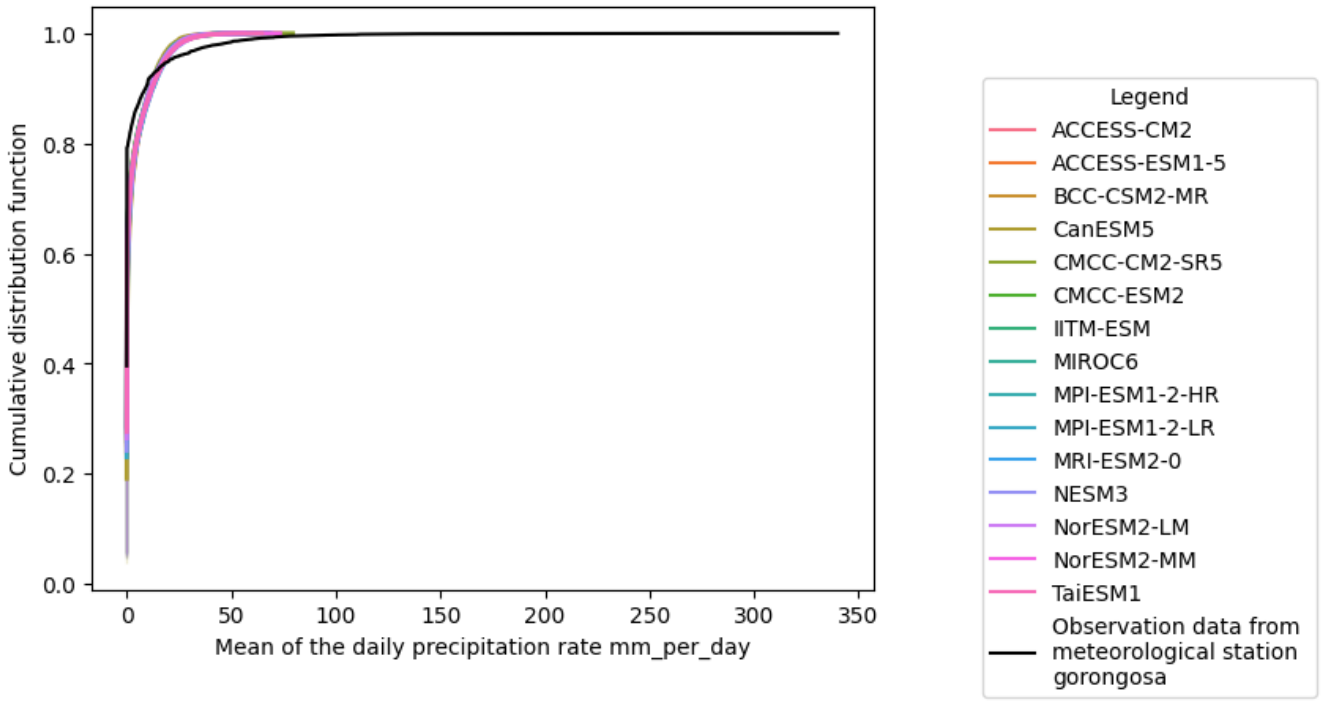

Figure 0-6 - CDFs of NEX-GDDP-CMIP6 modelled precipitation data mm/day, compared to CDF of observed precipitation data mm/day. All data are between 1980 and 2014 and are in Gorongosa. Each colored line represents the CDF for the output data of a GCM. The black line is the CDF of the observed data at the meteorological station in Chimoio. All models are following the same distribution, that does not comply with the observed distribution, particularly for extremes and low values.

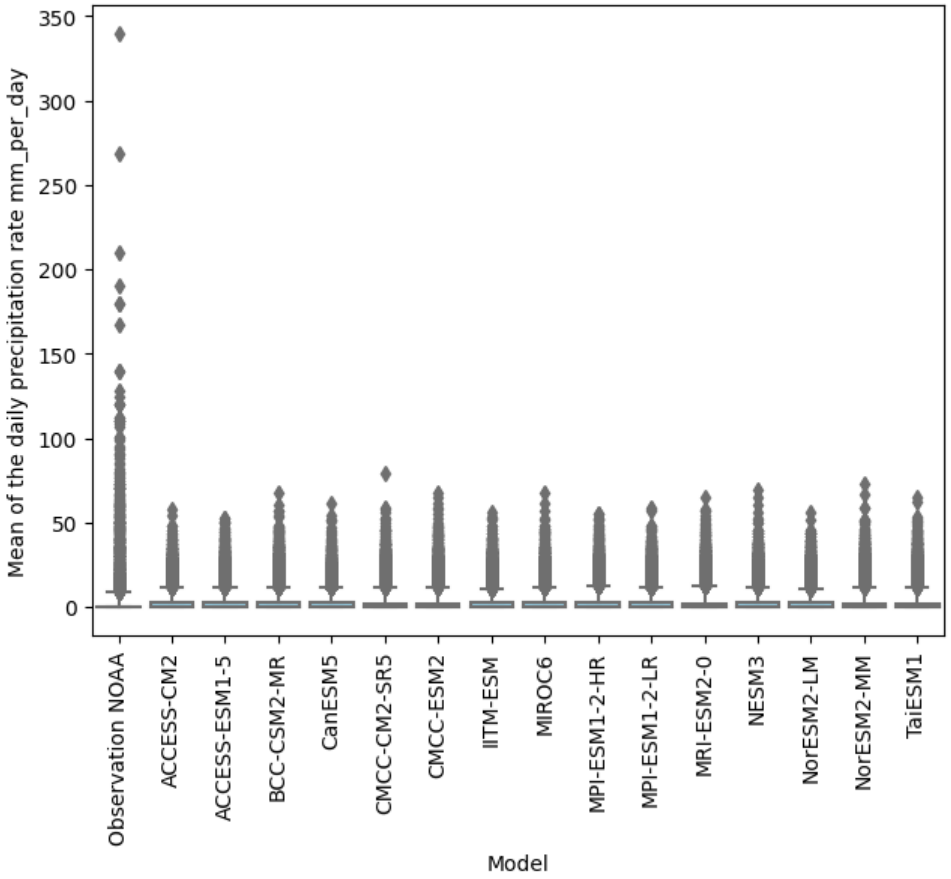

Figure 0-7 - Boxplots of the NEX-GDDP-CMIP6 modelled precipitation mm/day (in blue), compared to the boxplot of the precipitation mm/day registered by the meteorological station (in pink, first boxplot on the left). Data are between 1980 and 2014 and are from Gorongosa. The boxplots are presented with the median as the central line, the 25-th/75-th percentile as first and third quartile, the 10-th percentile and the 90-th percentile as whiskers and with outliers. The extreme modelled data are very small in comparison to the observed one.

Appendix C – Results vulnerability assessment with precipitation indicator

Table 0-1 - Statistical distribution for wet season during past period (1970-2014)

	Wet season monthly average precipitation mm							
	count	mean	std	min	10%	50%	90%	max
Name project								
Gorongosa_EIB	72.0	157.081061	75.285776	22.094667	30.367685	187.802709	234.631011	242.215202

Table 0-2 - Statistical distribution for wet season during future period (2030-2074)

	Wet season monthly average precipitation mm							
	count	mean	std	min	10%	50%	90%	max
Name project								
Gorongosa_EIB	288.0	146.783134	79.919321	8.003278	18.462754	168.041396	233.247465	274.943102

Table 0-3 - Exposure level for precipitation climate variable changes

	Exposure level	
	Extreme rainfall change	Incremental rainfall change
Gorongosa_EIB	No	No